R+1 9/21/99

REPORT DOCUMENTATION PAGE

AFRL-SR-BL-TR-99-

0272

1. AGENCY USE ONLY (Leave blank)	2. REPORT DATE	3. REPORT TYPE AND DATES COVERED

4. TITLE AND SUBTITLE

Ultra-thin Films for Opto-electronic Applications

5. FUNDING NUMBERS

F49620-96-1-0317

6. AUTHOR(S)

Naoya Ogata

7. PERFORMING ORGANIZATION NAME(S) AND ADDRESS(ES)

Foundation for Advancement of International Science
3-9-1 Amakubo, Tsukuba-shi,
Ibaragi-ken 305-0005 Japan

8. PERFORMING ORGANIZATION REPORT NUMBER

Final rport
August 1,1999

9. SPONSORING / MONITORING AGENCY NAME(S) AND ADDRESS(ES)

AFOSR/NL
801 N. Randolph Street, Suite 732
Arlington, VA 22203-1977

10. SPONSORING / MONITORING AGENCY REPORT NUMBER

19991130 032

11. SUPPLEMENTARY NOTES

12a. DISTRIBUTION / AVAILABILITY STATEMENT

Contributed to Thin Solid Films

Approved for public release; distribution unlimited.

12b. DISTRIBUTION CODE

13. ABSTRACT *(Maximum 200 Words)*

Optically active poly(thiophene) with a high stereregularity was synthesized for the first time by using a Rieke zerocovanlent zinc catalyst. An optically active polymer having more than 93% of Head-Tail linkages was obtained from 3(2(S)-2-methylbutoxy)ethyl)thiophene. Electrical and optical properties of the Head-to-Tail polymer were much superior to those of random-type polymer derived from thessame monomer and the third order non-liniarity k_3 reached a high value of 10^{-7}esu.

14. SUBJECT TERMS

Non-linear optical polymer

15. NUMBER OF PAGES

16. PRICE CODE

17. SECURITY CLASSIFICATION	18. SECURITY CLASSIFICATION OF THIS PAGE	19. SECURITY CLASSIFICATION OF ABSTRACT	20. LIMITATION OF ABSTRACT

FACULTY OF PHOTONICS
SCIENCE AND TECHNOLOGY

CHITOSE INSTITUTE OF
SCIENCE AND TECHNOLOGY

858-65, Bibi, Chitose
Hokkaido 066-8655 JAPAN
PHONE : (81)123-27-
F A X : (81)123-27-

August 1, 1999

Dr. Charles Lee

AFOSR/NL
801 N. Randolph Street, Ste 732
Faiurfax, VA 22203-1977
U.S.A.

Dear Dr. Lee:
Enclosed I am sending the final report for the grant on "Ultra-thin Films for Opto-electronic Applications".
I thank you very much for your strong support on our research.
With my best regards,

Naoya Ogata
President and Professor
Chitose Institute of Science and Technology

Final Report to AFOSR

Title of Research Grant: **Ultra-thin Films for Opto-electronic Applications**

Principal Investigator: Naoya Ogata, Professor Emeritus
Foundation for Advancement of International Science
3-9-1 Amakubo, Tsukuba-shi, Ibaragi-Ken 305-0005,
Japan
Tel: +81-298-51-1221 Fax:+298-51-9440

Naoya Ogata

Research Period: **June 14, 1998-June 15, 1999**

Date of Report: **August 1, 1999**

Abstract

Optically active poly(thiophene) with a high regioregularity was synthesized for the first time by using a Rieke zerovalent zinc catalysts. *Head to Tail* Poly(3-[2((S)-2-methylbutoxy)ethyl]thiophene (*HT*-P(S)MBET) was an optically active polymer with more than 93% of the *Head-to-Tail* linkages. For comparison purposes, regiorandom *R*-P(S)MBET and achiral *HT*-P(±)MBET were also synthesized. They are fully characterized by using proton and carbon 13 NMR spectroscopies, optical rotatory power measurements, circular dichroism, gel permeation chromatography and UV-Vis spectroscopy.

Both electrical conductivities and third-order optical nonlinearities were measured in order to examine opto-electronic properties of these ultra-thin films. It was suggested that electrical and optical properties were little affected by chirality. An anisotoropies of electrical conductivity for *HT*-(P)MBET/SA mixed LB films were in close agreement with results of structural analyses. The electrical and optical properties of *HT*-P(S)MBET/SA LB films were superior to those of spin-coated films. From these results, it was concluded that the regioregular poly(thiophene)s enhanced opto-electronic properties owing to the extended conjugation length of main polymer chains.

Background

The presence of various substituents on the poly(thiophene) backbone can not only modify the processibility but also modulate the electrical and optical properties of the resulting polymers. Therefore, it is important to synthesize and characterize novel poly(thiophene) derivatives. At the same time, it is necessary to make sure whether or not the synthetic method already known can be applied to uninvestigated compounds.

Recently, a number of studies on synthesis and applications of head-to-tail regioregular poly(3-alkylthiophene)s have been reported. [1-10] Regioregularity has been identified to be the one of the most significant factors that influence the physical structure and properties of polymers. Structurally homogeneous, regioregular poly(3-alkylthiophene) can be obtained by the Rieke method [3-4] already described in chapter 1. So far, a number of papers have been published concerning the syntheses of regioregular poly(3-substituted thiophene) [11-18]. However, there have been no reports about the preparation of regioregular poly(thiophene) derivatives with optically active units by the Rieke method.

In the present study, chiral poly(thiophene) with the high regioregularity was synthesized by the modified Rieke method for the first time. The regioregularity of polymers prevented the conjugated structure from structural defects and gave self-organization. Regioregularity of chiral polymer can be also expected to bring out full potential caused by the optically active side chain.

In this chapter, the syntheses and characterizations of the poly(thiophene) derivatives (**Figure 3.1**) will be described.

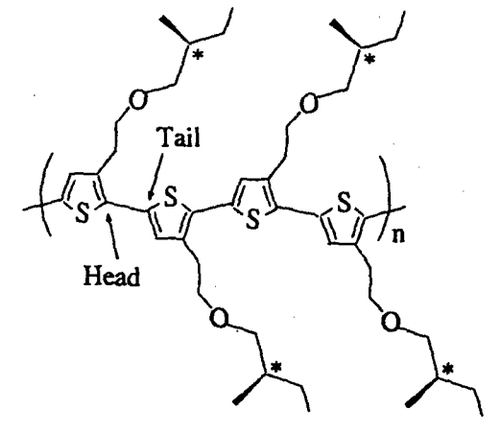

HT-P(S)MBET

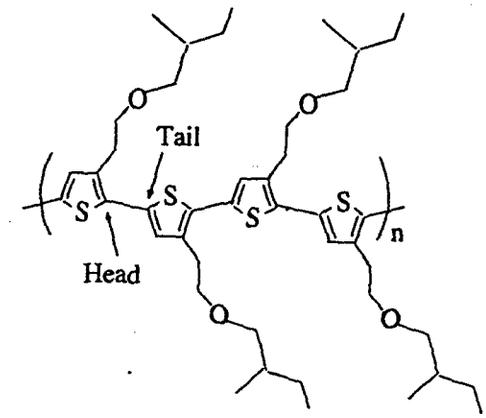

HT-P(±)MBET

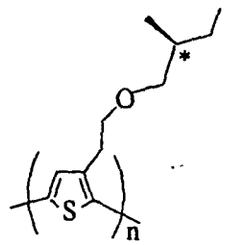

R-P(S)MBET

Figure 3.1. Structures of the polymers used in this study

3-2. Syntheses of Polymers

The syntheses of head-to-tail type polymers and its intermediates were performed according to **Scheme 2.1-2.2.**

A 2,5-dibromothiophene derivative monomer (DBr-(S)MBET) was synthesized from (S)-(-)-2-Methyl-1-butanol, which is commercially supplied and widely used as an optically active building block. This alcohol was treated with p-TsCl to get reactive intermediate p-toluenesulfonate. The thiophene monomer((S)MBET) could be obtained by the reaction of *p*-toluenesulfonate with 2-(3-thienyl)ethanol in the presence of KOH by using Williamson ether synthesis. Bromination of (S)MBET with NBS afforded DBr-(S)MBET in good yield.

The Rieke method [3-4] was used as the polymerization method. This is a one-pot reaction, while the McCllough method [1-2] is a one pot, multistep procedure. One advantage of the Rieke method is that highly reactive Zinc affords a functional-group-tolerant synthesis. The Rieke zero valent zinc is very sensitive to the moisture in the air. Therefore, all operations were conducted in a argon atmosphere. Special attention was paid to dryness of apparatus and purity of the starting monomer DBr-(S)MBET. **Scheme 3.1** depicts the regiocontrolled synthesis of *HT*-P(S)MBET using highly reactive metal powder, Rieke zinc (Zn*). Zn* underwent direct oxidative addition to DBr-(S)MBET chemoselectively to form a 2-bromo-3-substituted-5-(bromozincio)thiophene predominantly. No bis(bromozincio)thiophene was formed. This regioselectivity of the oxidative addition is a unique advantage of Rieke zinc, providing a convenient route for the specific synthesis of regioregular organometallic reagents. Ultrasonication was used for activation of zinc surface. [19]

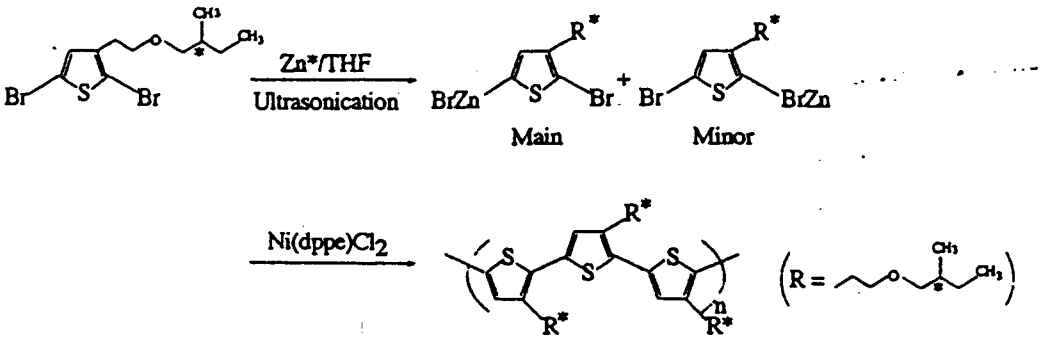

Scheme 3.1. Regiocontrolled synthesis of Head-to-Tail poly (3-[2-((S)-2-methyl butoxy)ethyl]thiophene) (*HT*-P(S)MBET) mediated by Rieke zinc.

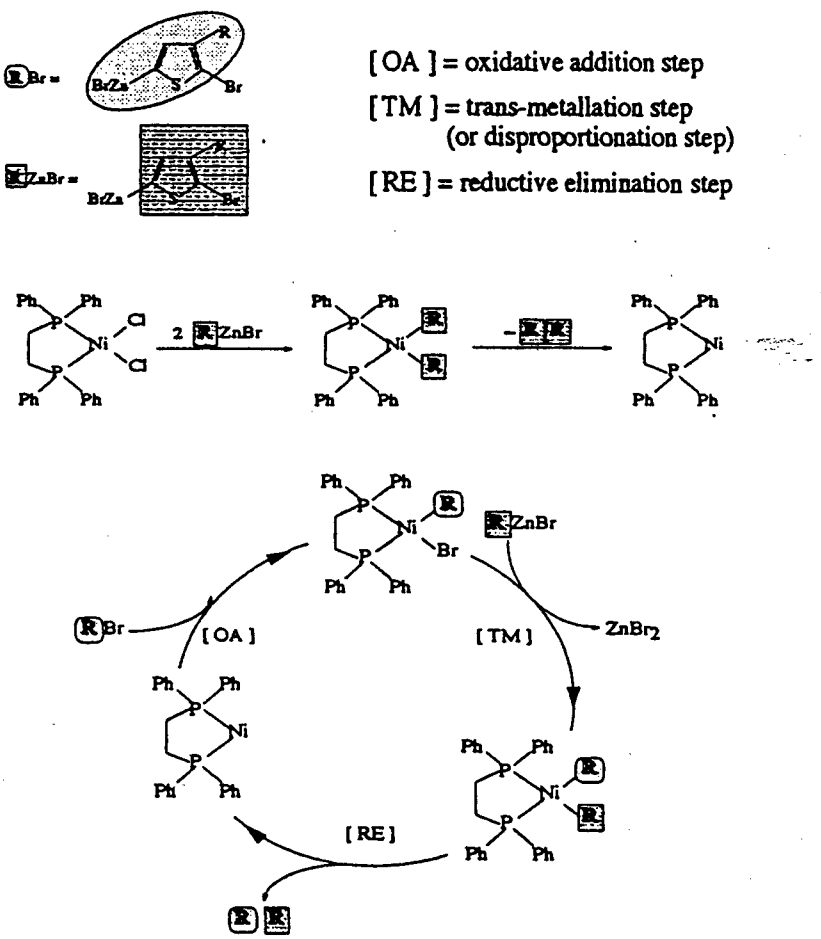

Scheme 3.2. Regiocontrolled polymerization mechanism by $Ni(dppe)Cl_2$.

Usually, a metal surface is not pure. A solid coating of oxides, hydroxides, and carbonates, constitutes a "passivation" layer which prevents the reagent in the solution from reaching the metal. By using Ultrasonication, it was expected that the surface of Zn* was activated and that catalytic activity is increased. It was also reported that Rieke zinc was sonochemically prepared. [20] The addition of a Ni cross-coupling catalyst led to the formation of a regioregular *HT*-P(S)MBET. **Scheme 3.2** may serve as a working hypothesis for nickel-catalyzed cross-couplings. [21] The cast film of *HT*-P(S)MBET was a flexible, deep purple-colored film with a metallic luster. The achiral *HT*-P(±)MBET was synthesized by the same procedure and condition for the comparison with the *HT*-P(S)MBET. The color of *HT* -P(±)MBET cast film was also deep purple with a metallic luster.

The attempts to synthesize regiorandom *R*-P(S)MBET by chemical oxidative methods have been unsuccessful. In generally, regiorandom poly(3-alkylthiophene)s with good solubility were easily prepared by oxidative coupling of 3-alkylthiophene with ferric (III) chloride in chloroform. (**Scheme 1.1**) [22-23] This method usually yields regio random polymers with 60-70 % HT couplings. In the case of 3-[2-((S)-2-methylbutoxy)ethyl]thiophene, *R*-P(S)MBET obtained by this method was insoluble in typical organic solvents. The reason of this insolubility is crosslinking through the side chain. In a recent study a comparison has been made between the polymerization of 3-substituted thiophene and its deuterated analogue, indicating that considerable crosslinking occurs through the side chain. [24] The degree of crosslinking depends on the structure of the monomer. The degree reduced by performing the reaction at temperatures below -20 °C which also increases the yield of

soluble polymer. According to many other reports, every possible condition was tried (for example, low temperature [25], low oxidation potential [26]). Even if the reaction condition of -40 °C was used, crosslinking occurs through the side chain and the resultant polymer was not soluble.

Therefore, in order to obtain regiorandom polymers with good solubility, *R*-P(S)MBET was prepared with Rieke zinc, followed by catalytic polymerization with $Pd(PPh_3)_4$. **(Scheme 2.3)** It was reported that the degree of regioregularity of poly(3-alkylthiophene) was a function of both metal and ligands of the catalysts in polymerizations. [4] Switching the catalyst from $Ni(dppe)Cl_2$ to $Pd(PPh_3)_4$ led to a reduction in the regioregularity. The catalyst with the greatest steric congestion, $Ni(dppe)Cl_2$, produces almost exclusively cross-coupled products. On the contrary, the catalyst with the least congestion, $Pd(PPh_3)_4$, produces a random mixture of cross- and homocoupled product. By using $Pd(PPh_3)_4$, regioirregular *R*-P(S)MBET with good solubility was obtained. The *R*-P(S)MBET cast film was very sticky compared to *HT*-P(S)MBET. The cast film of *R*-P(S)MBET was a red-brown, transparent film.

3-3. Characterizations of Polymers

Structures of the resultant polymers used in this study are shown in **Figure 3.1**. They are fully characterized using ^{1}H- and ^{13}C-NMR spectroscopy, optical rotatory power measurements, circular dichroism (CD), gel permeation chromatography (GPC) and UV-Vis spectroscopy.

Structures of the polymers used in this study were determined by ^{1}H, ^{13}C, H-H cosy, and C-H cosy NMR spectroscopy in detail. The ^{1}H and ^{13}C NMR spectra of regioregular *HT*-P(S)MBET and regioirregular *R*-P(S)MBET are shown in **Figures 3.2** and **3.3**, respectively. Achiral polymer, *HT*-P(±)MBET, showed the same NMR spectra as chiral *HT*-P(S)MBET. The structural regularity of the polymers was also examined by ^{1}H -NMR and ^{13}C-NMR spectroscopies. [27] Since the resultant polymers are soluble in common organic solvents such as chloroform and tetrahydrofuran, NMR can be used to determine their structure and regiochemistry. The ^{1}H- and ^{13}C-NMR spectra of poly(3-substituted thiophene)s provide sensitive probes for the substitution pattern in the polymer backbone. The proton in the 4-position of the thiophene ring experoences four different chemical environments in a mixture of four possible triad regioisomers. These four chemical shift in aromatic region are uniquely distinguishable by NMR spectroscopy. For example, ^{1}H-NMR spectra of the regioregular poly(3-hexylthiophene) show four singlets in the aromatic region that can be clearly attributed to the protons on the 4-position of the central thiophene ring in each configurational triad : HT-HT(δ = 6.98), TT-HT(δ = 7.00), HT-HH(δ = 7.02), TT-HH(δ = 7.05). [2,4]

As shown in **Figure 3.4**, the ^{1}H NMR spectrum of the *HT*-P(S)MBET shows a single peak in aromatic region (δ = 7.10) assigned to the

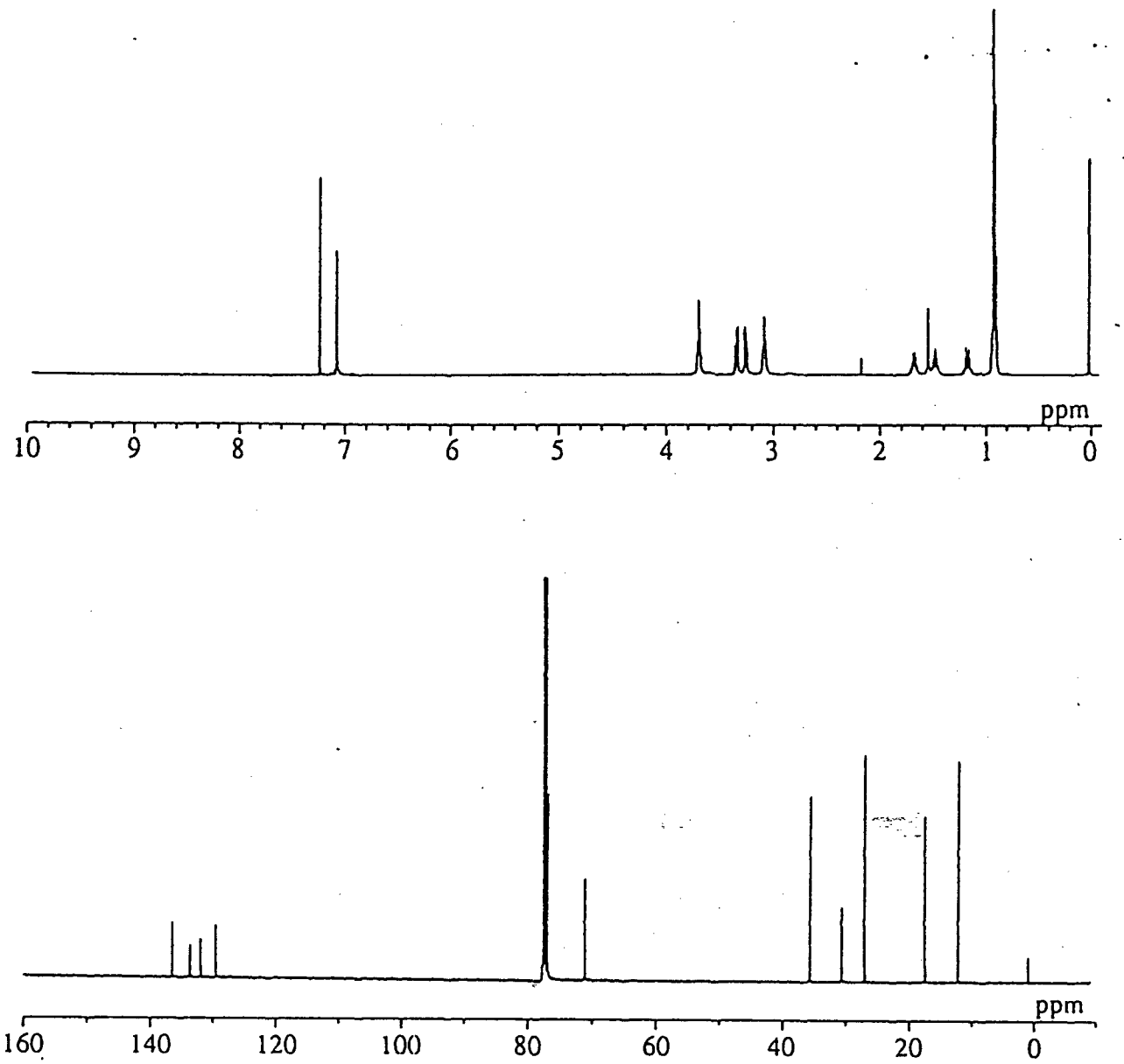

Figure 3.2. ^{1}H and ^{13}C NMR spectra of *HT*-P(S)MBET in $CDCl_3$.

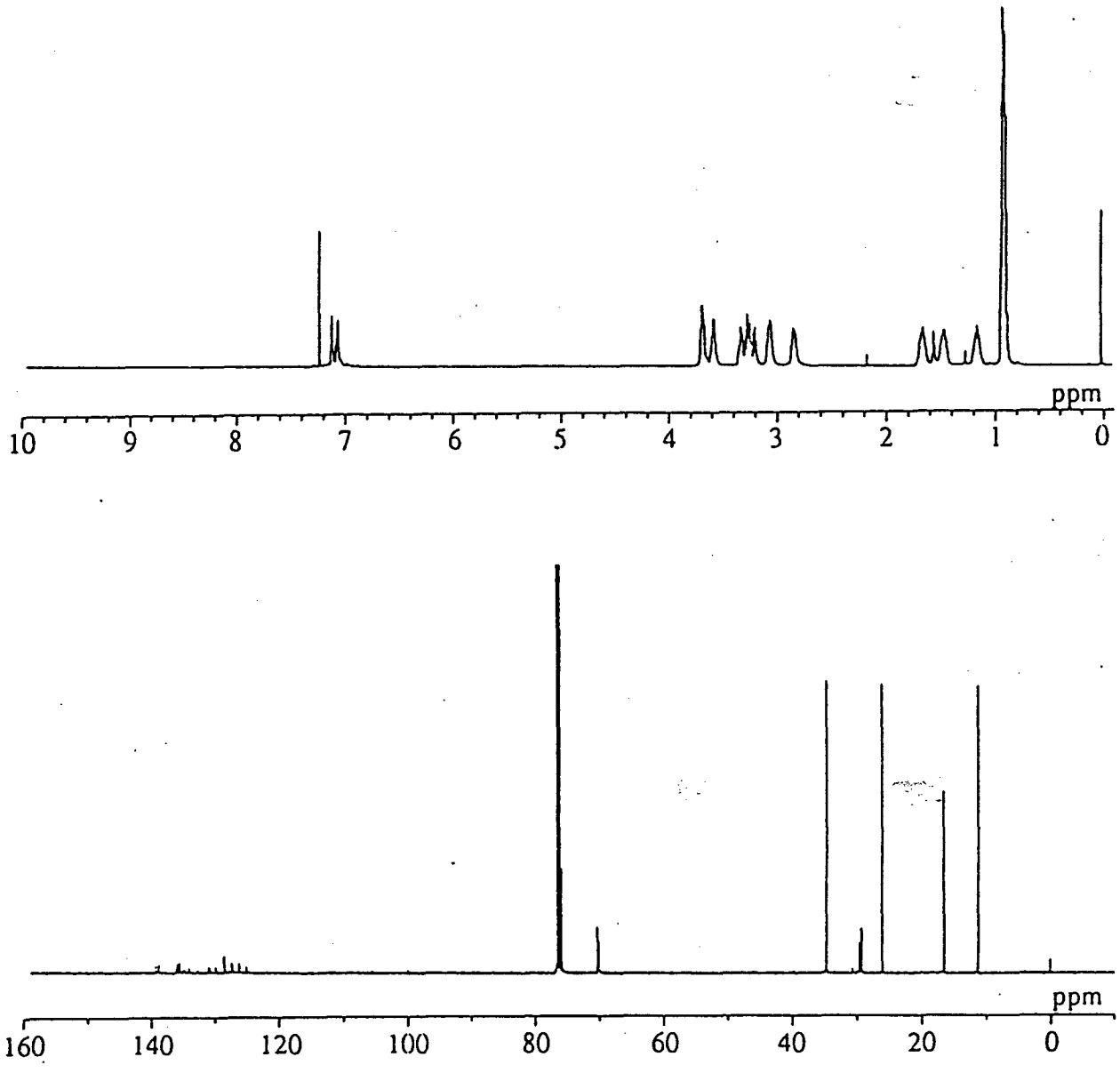

Figure 3.3. ^{1}H and ^{13}C NMR spectra of *R*-P(S)MBET in $CDCl_3$.

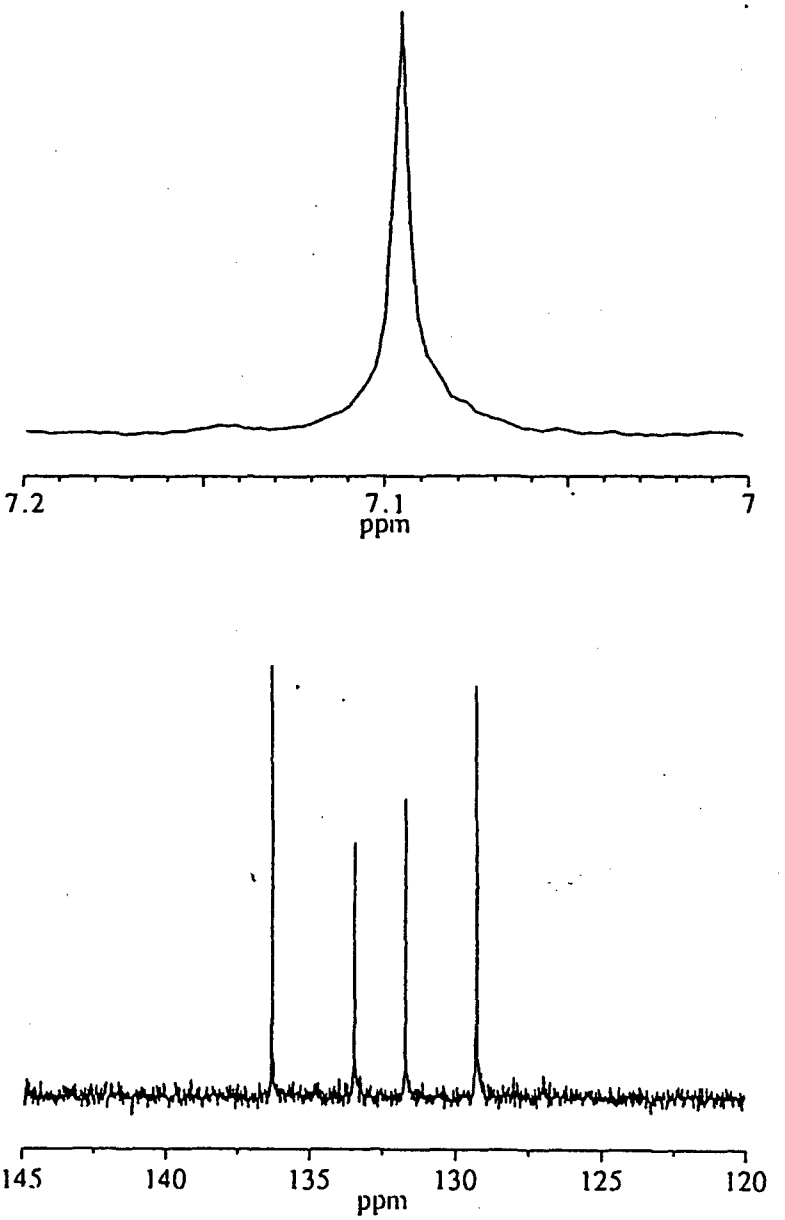

Figure 3.4. Expanded ^{1}H and ^{13}C NMR spectra of *HT*-P(S)MBET in $CDCl_3$.

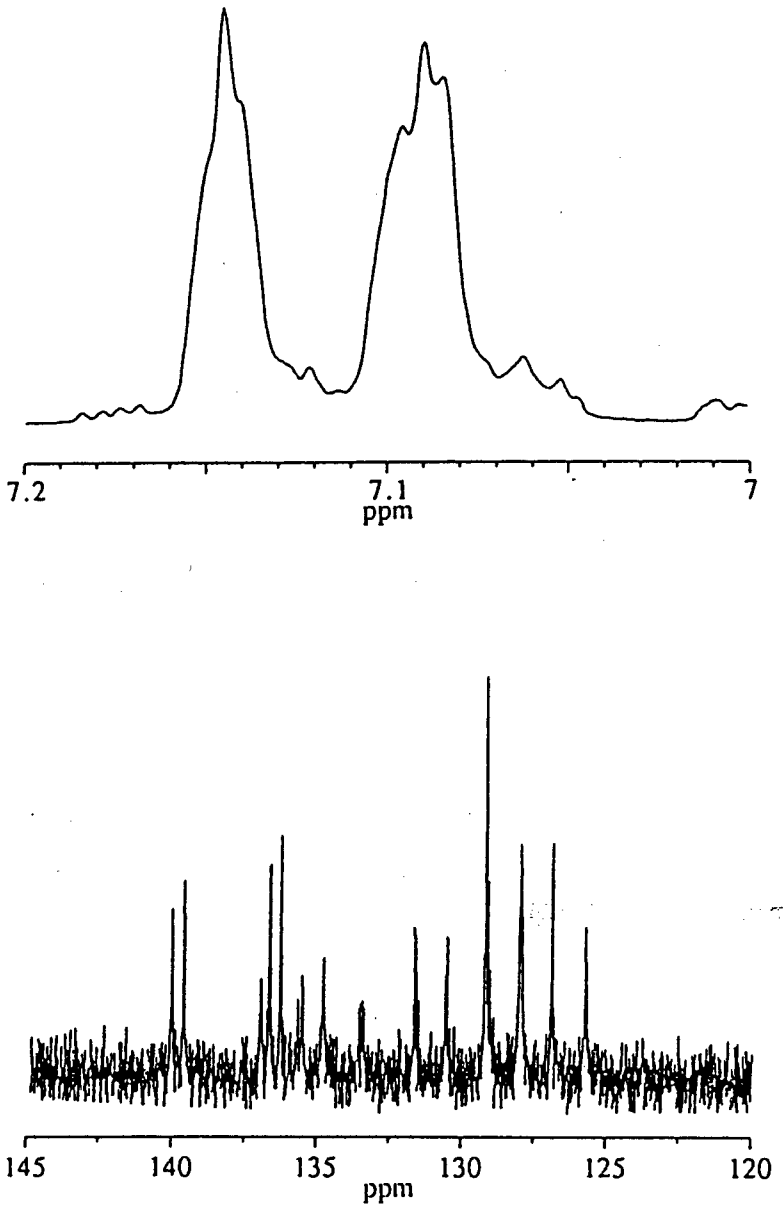

Figure 3.5. Expanded ^{1}H and ^{13}C NMR spectra of *R*-P(S)MBET in $CDCl_3$.

proton at the 4-position of the HT-coupled thiophene rings. The spectrum of *HT*-P(S)MBET does not indicate the presence of any regioisomers. This result was clearly confirmed by the ^{13}C NMR spectrum. Only four sharp peaks (δ =130-140) for the carbon atoms of an HT-coupled thiophene ring are observed in the ^{13}C NMR spectrum.

In contrast, for regiorandom *R*-P(S)MBET, there are several peaks (mainly δ = 7.10 and 7.20) in the aromatic region that can be attributed to the protons on the 4-position of the central thiophene ring. (**Figure 3.5**): From this spectral data, it seems that *R*-P(S)MBET are regiorandom, as they contain almost equal amounts of HT and HH configurations. In the ^{13}C NMR spectrum, all of the thiophene carbons (16 peaks are theoretically possible) can be resolved in the mixture of the four triad regioisomers.

The relative ratio of HT-HT couplings to non-HT-HT couplings can be also determined be the analysis of the protons that are the α-carbon of the 3-substituent on thiophene. Relative integration of the HT-HT peak relative to the other non-HT resonances can give the percentage of HT-HT couplings. The head-to-tail ratio of the *HT*-P(S)MBET was estimated from the α-methylene proton as more than 93%. The *HT*-P(S)MBET prepared by this procedure is as regioregular as poly(3-alkylthiophene)s obtained by the Rieke method. On the other hand, the head-to-tail ratio of the *R*-P(S)MBET was estimated from the α-methylene proton as 54%. The head-to-tail ratio and yield of each polymer are included in **Table 3.1**. Though the yields were relatively lower (21.8 % - 30.5 %) than those of poly(3-alkylthiophene)s, it was found that the thiophene derivatives containing optically active units and oxygen atoms on the side chain could be polymerized by the Rieke method.

Table 3.1. Yields of polymerization and Head-to-Tail contents of polymers.

Polymer	Yield (%)	HT content (%)
HT -P(S)MBET	30.5	> 93
HT -P(±)MBET	21.8	> 96
R -P(S)MBET	24.1	54

Table 3.2. Molecular weights and related properties of polymers.

Polymer	Mw	Mn	Mw / Mn	Xn
	g / mol			
HT -P(S)MBET	23,700	15,500	1.52	121
HT -P(±)MBET	22,300	13,600	1.64	114
R -P(S)MBET	20,500	10,160	2.02	104

Molecular weights of the polymers were experimentally determined by GPC. During the polymerization process in which these large macromolecules are synthesized from smaller molecules, not all polymer chains will grow to the same length. This results in a distribution of chain lengths or molecular weights. **Table 3.2** shows the number-average molecular weight M_w, the weight-average molecular weight M_n, and polydispersity index $D = M_w / M_n$ of the polymers synthesized in this study. Molecular weights was M_n = 20.5-23.7 k g/mol with narrow weight distributions of 1.52-2.02. The number of the monomer units in one chain was in the range of 104-121. It was noted that molecular weights of these polymers are nearly equal and that the comparison of properties is possible. In addition, it is well known that the chemically synthesized materials have rather high D ranges, typically from 2.0 to 5.0. Therefore, a value of 1.5-2.0 is considered to be very good. Materials with large D values will contain chains of strongly varying lengths, and when these chains enter the crystalline regions each chain termination will disrupt the organization into well-defined lattices and thus will affect the crystallinity.

The optical rotations of the chemicals in chloroform at the sodium D-line are also shown in **Schemes 2.1** and **2.2**. In **Scheme 2.1**, all the chemicals possess optical rotatory power, indicating that no racemization took place at any time during any reaction. In addition, the $[\alpha]_{589}^{23}$ of the *HT*-P(S)MBET in chloroform was induced up to 7700 by adding a poor solvent (Methanol). As pointed out by Meijer et al., this means that the *HT*-P(S)MBET changes from the disordered non-planar structure to coplanar associated structure in poor solvents. [17]

A qualitative measure of π-orbital overlap in solution can be probed by UV-Vis absorption spectroscopy. In conjugated polymers, the extent of conjugation length directly affects the observed energy of the absorption. Therefore, UV-Vis spectroscopy provides an important method by which the conformational state and structure of π-conjugated polymers may be observed. An increase in maximum absorption wavelength (λ_{max}) is evidence for increased coplanarity and longer π-conjugation length.

The polymers were soluble in chloroform and the existence of π–conjugation in these polymers was implied by their solution colors (bright yellow). **Figure 3.6** shows the UV-Vis absorption spectra of chiral polymer *HT*-P(S)MBET and racemic polymer *HT*-P(±)MBET in chloroform. The head-to-tail ratios of these polymers were estimated as > 93% and can be regarded as almost the same. The experiment in this study was carried out by using very dilute polymer solutions in chloroform. Therefore, solubility was not a problem. The spectra of these polymers are virtually identical. The addition of the optically active side chain, as is well known, does not cause any significant changes in the UV-Vis spectra. The onset of absorption occurs at about 600 nm (2.06 eV) and the peak is at about 444 nm (2.79 eV).

The UV-Vis absorption spectra of of regioregular *HT*-P(S)MBET and regiorandom *R*-P(S)MBET in chloroform are shown in **Figure 3.7.** The maximal absorption is the π–π* transition for the conjugated polymer backbone. As shown in this figure, UV-Vis absorption spectrum of *HT*-P(S)MBET in chloroform showed lower transition energy than those of regioirregular *R*-P(S)MBET, although the molecular weight of *HT*-P(S)MBET is almost the same as those of *R*-P(S)MBET. The regioregular *HT*-P(S)MBET has a maximum absorption wavelength at 444 nm (2.79

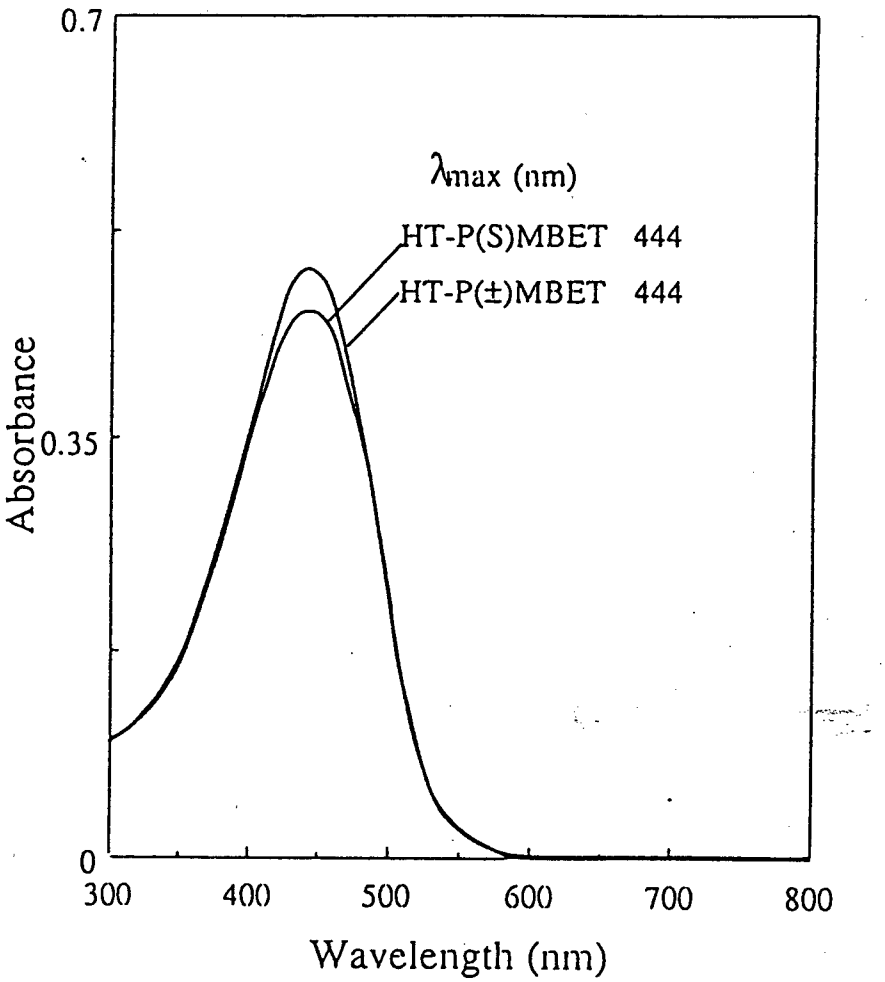

Figure 3.6. UV-Vis absorption spectra of *HT*-P(S)MBET and *HT*-P(±)MBET in chloroform solutions.

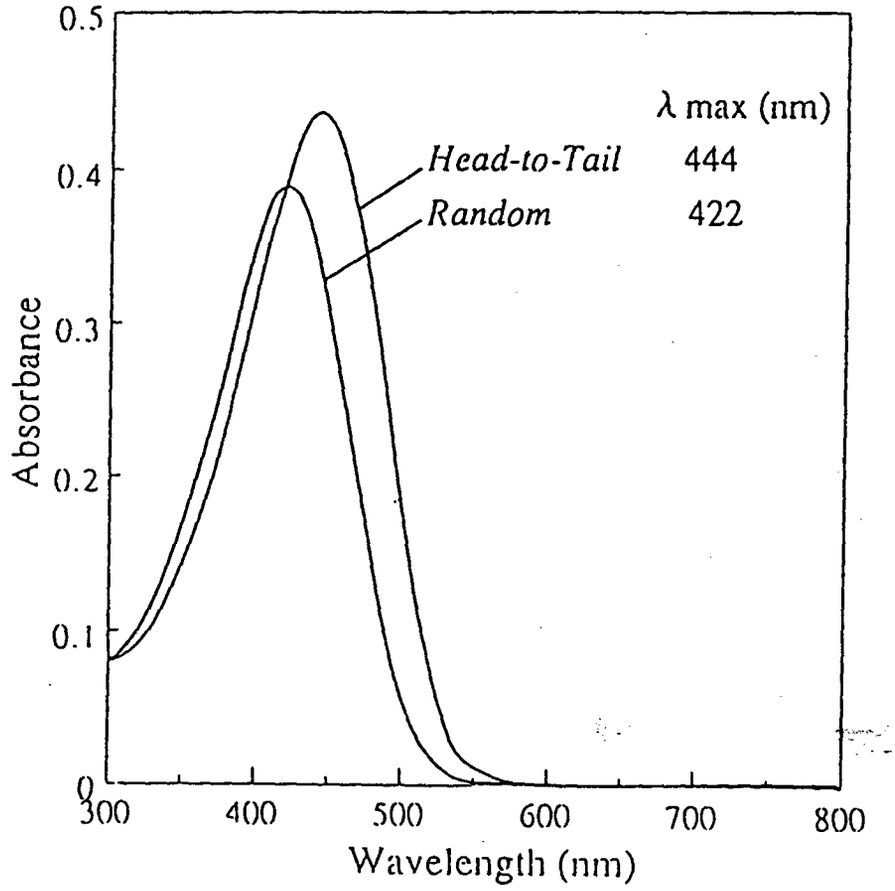

Figure 3.7. UV-Vis absorption spectra of *HT*-P(S)MBET and *R*-P(S)MBET in chloroform solutions.

eV),which is 22 nm (0.15 eV) longer than regiorandom *R*-P(S)MBET with a λ_{max} of 422 nm (2.94 eV). As the literature indicated [28], the poly(3-substituted thiophene) in solution has two conformations: rod-like and coil-like. The more rod-like conformation resulted from the longer conjugation length along the main chain. This suggests that in solution the main chain of regioregular *HT*-P(S)MBET has a more planar (rod-like) conformation with longer effective conjugation length, while the main chain of regiorandom *R*-P(S)MBET has a more non-planar (coil-like) conformation with shorter effective conjugation length.

A microstructural irregularity of *R*-P(S)MBET creates a sterically driven twist of the thiophene rings out of coplanarity and conjugation with one another. This is illustrated by the schematic view in **Figure 3.8**. The larger the torsion angle between thiophene rings, the larger the bandgaps will be in poly(thiophene) as compared to a structure with well-defined head-to-tail chemistry. In regioregular *HT*-P(S)MBET, steric repulsions between the side chains on the thiophene ring will be decreased, thereby increasing the effective conjugation length between thiophene rings.

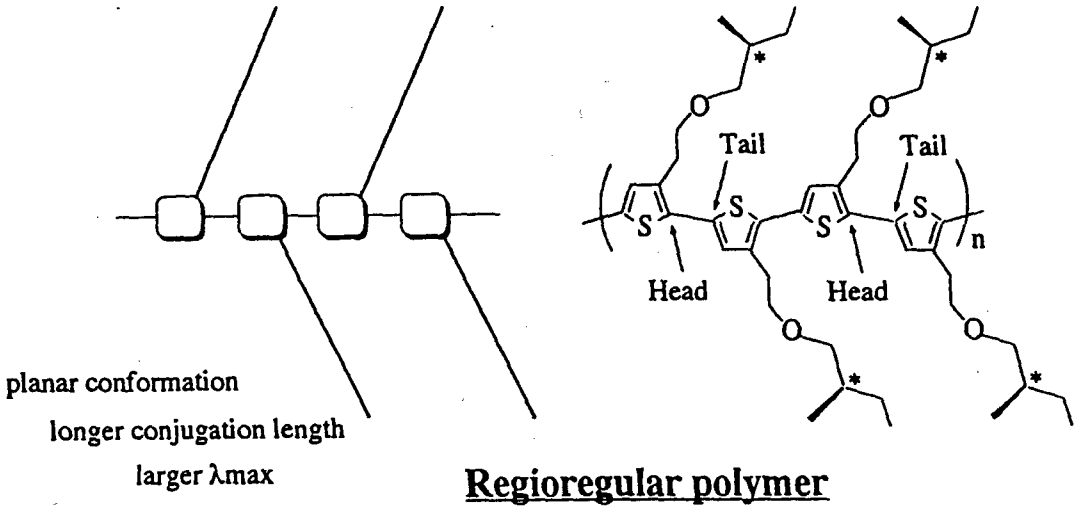

Regioregular polymer

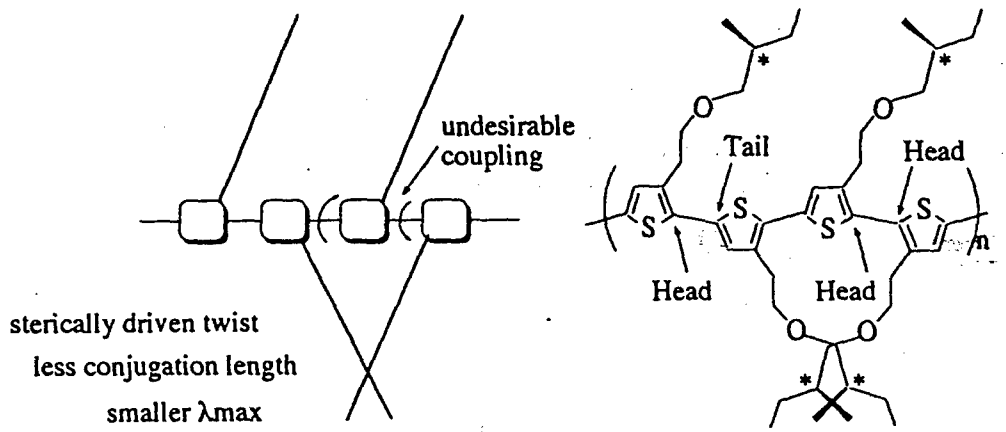

Regiorandom polymer

Figure 3.8. Schematic view of the thiophene rings for regioregular and regiorandom poly(thiophene)s.

On the other hand, enantiomerically pure side chains can afford chiral semi-conducting polymers that exhibit circular dichroism (CD), the difference in absorption of right and left circularly polarized light, in the UV-Vis absorption region. The chirality of the main chain of *HT*-P(S)MBET and *R*-P(S)MBET was examined with CD in a chloroform / methanol solution at room temperature. The CD in these chiral conjugated materials is strong when the polymer chains are in an aggregated phase, such as in a solid film or microcrystalline which is formed by adding a poor solvent. The CD spectra of these polymers in chloroform / methanol solutions are shown in **Figures 3.9.** The CD spectra of the chiral *HT*-P(S)MBET and racemic *HT*-P(±)MBET are given in **Figure 3.9(a).** Racemic polymer *HT*-P(±)MBET does not exhibit circular dichroism. In contrast, chiral polymer *HT*-P(S)MBET has strong negative Cotton effects at about 560 nm and 610 nm. The CD spectra of the *HT*-P(S)MBET and *R*-P(S)MBET are given in **Figure 3.9(b).** Regiorandom *R*-P(S)MBET in a mixed solution does not exhibit circular dichroism in its UV-Vis absorption region (300-550 nm). Due to the more extended π-conjugated system, regioregular *HT*-P(S)MBET shows significantly increased CD effect compared with regioirregular *R*-P(S)MBET. The observation is in accordance with that by Bouman and Meijer et al. and supports the fact that regioregularity is an important factor in the development of chiral structure. [17]

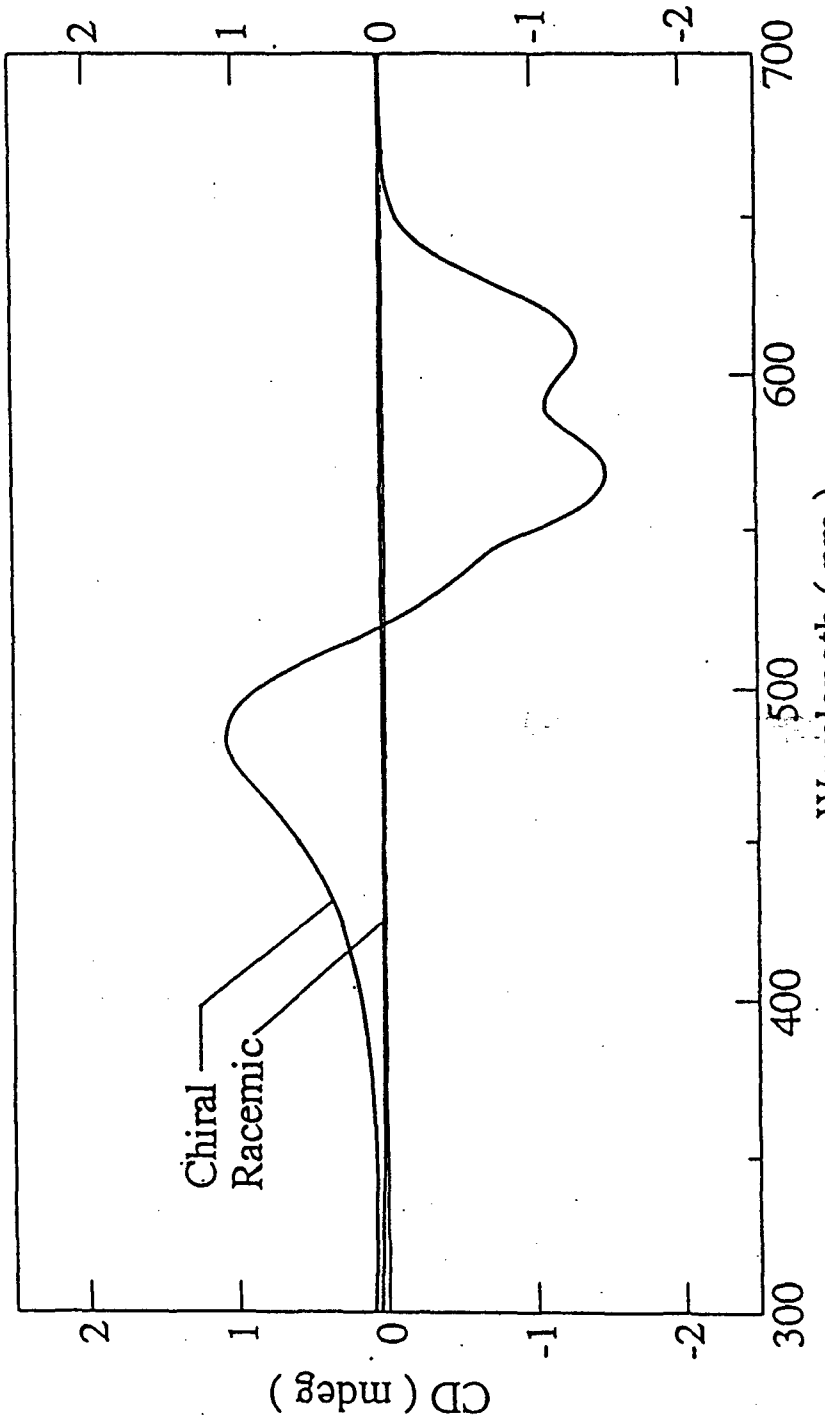

Figure 3.9. CD spectra of polymers in $CHCl_3$ / MeOH (1/1) solutions.

3-4. Thermochromism

The strong interaction between electronic structure and backbone conformation is a unique feature of conjugated polymers. Because of this reason, the study of conjugated polymers in solution is interesting, since in such systems conformational changes are coupled to the electronic states of the π electron system. Dramatic color changes (chromism) associated with changes in conformation are therefore expected. By changing the temperature (or by adding non-solvent to the polymer solution), there is a shift of the optical absorption features. For example, the polymer in the good solvent such as chloroform is yellow. In this case, the chain structure has been described either as a random coil or a worm like chain. The yellow solutions display a dramatic color change (yellow to magenta) on addition of a poor solvent (solvatochromism) or on cooling to low temperatures (thermochromism). This transition has been associated with formation of extended polymer chains as a result of aggregation. This is also a reversible transition.

Poly(thiophene) without substituents does not show any chromism, since the coiling of the side chains drives the torsion of the main chain. The molecular structure of poly(3-substituted thiophene) is crucial to chromic phenomena.[29] The chemical structure and size of the substituent and the regularity of substitution influence the character of the chromic transition. Here, I investigated thermochromic phenomena of poly (thiophene) derivatives.

Figure 3.10 shows the absorption spectra of *HT*-P(S)MBET in a chloroform / alcohol ((s)-(-)-2-methyl-1-butanol) (9/1) mixed solution (1mg / 100ml solvent) recorded at various temperatures. The solution

color at 10 °C is magenta. Chloroform is good solvent, whereas alcohol is bad solvent. On heating, a significant thermochromism is observed and a yellow solution is obtained. The absorption maximum at 600 nm was shown to decrease in intensity with increasing temperature. This was attributed to a loss of planarity and conjugation induced by thermal disturbance. It is generally accepted that, at low temperature, adjacent thienyl units adopt a trans-planar conformation which favors a longer conjugation length and a red-shifted absorption maximum. At elevated temperatures, the trans-planar conformation of the side chains is less stable and a trans to gauche conversion occurs. This conversion forces the thiophene rings along the main chain to twist with respect to each other, resulting in a coiled chain with shorter conjugation length and a corresponding blue shift of the absorption maximum.

Figure 3.11 shows temperature-dependent UV-Vis absorption spectra of *HT*-P(S)MBET in a chloroform / alcohol ((±)-2-methyl-1-butanol) (9/1) mixed solution. When racemic alcohol, (±)-2-methyl-1-butanol, was used as poor solvent, the rate of blue shift was slightly faster. That is to say, it was shown that thermochromic phenomenon was slightly affected by chirality. It was suggested that the aggregation of *HT*-P(S)MBET was easily maintained when chiral (s)-(-)-2-methyl-1-butanol was used as poor solvent. This is an agreement with the result that *HT*-P(S)MBET exhibits homochiral behavior in temperature-dependent π-A isotherms (chapter 4).

These studies have also revealed interesting feature. The presence of broad isosbestic points in **Figure 3.10** and **3.11** is surprising, since a progressive conformational change should lead to a progressive blue shift of the absorption spectra. The presence of the broad isosbestic point

indicates that a progressive conformational change of the backbone does not take place in regioregular poly(thiophene) derivatives. I have interpreted the presence of the isosbestic point in the temperature-dependent absorption spectra by the equilibrium between two major conformers. It is suggested that there is an equilibrium between two populations of conformers, one population centered at a more twisted conformation at high temperatures and another centered at a more planar conformation at low temperatures. Recently a similar isosbestic point have been reported for poly(thiophene).

On the other hand, **Figure 3.12** shows the temperature-dependent absorption spectra of regiorandom *R*-P(S)MBET in a chloroform / alcohol ((s)-(-)-2-methyl-1-butanol) (9/1) mixed solution. The solution color at 10 °C is yellow even if in mixed solution. On heating, a significant thermochromism is not observed. *R*-P(S)MBET exhibits weak and monotonic shifts of their absorption maximum. This is because the steric hindrance is already close to maximal, and will not increase on heating. As observed with regiorandom polymer *R*-P(S)MBET, if the steric interactions are too large, no planar conformation is accessible and polymer is not thermochromic. In regiorandom *R*-P(S)MBET, an isosbestic point was not observed. Only localized conformational defects can be created along the backbone, leading to a monotonic blue shift in the absorption maximum upon heating.

It was found that the regioregularity of substitution is important to chromic phenomenon.

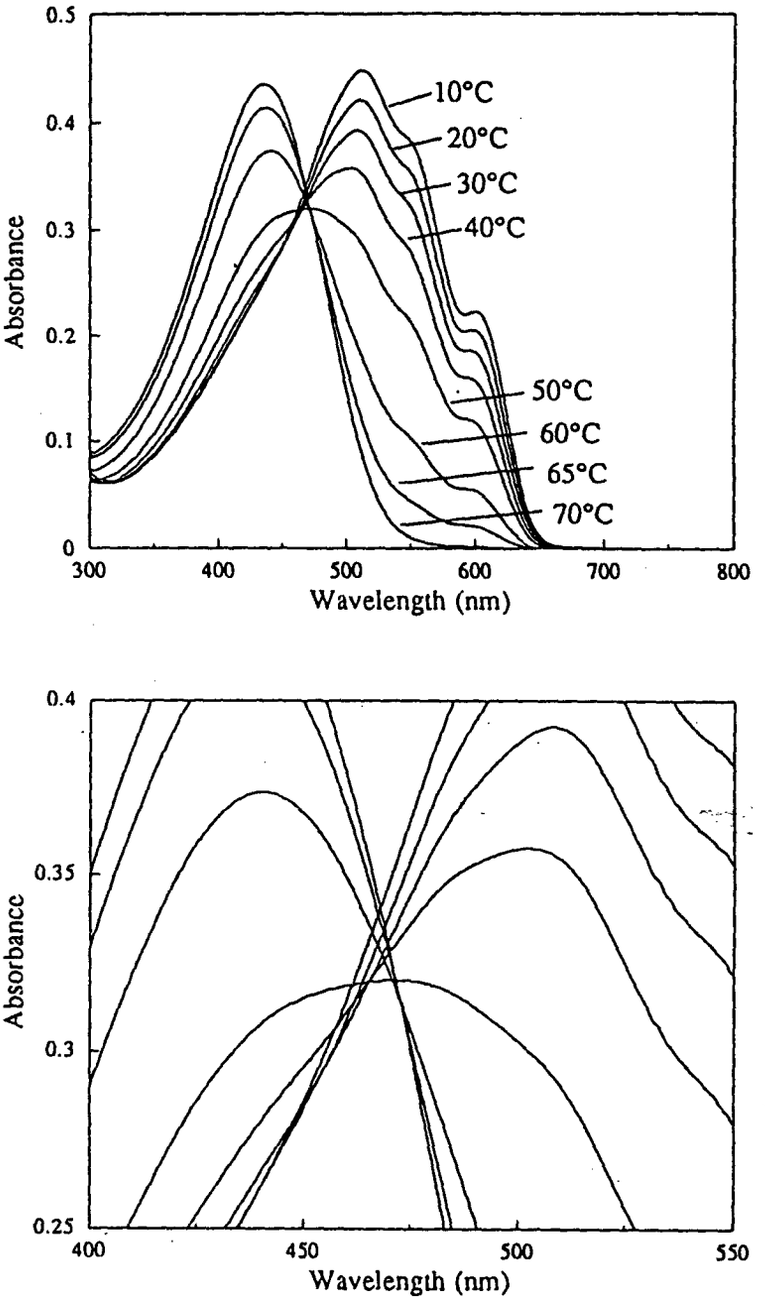

Figure 3.10. Temperature-dependent UV-Vis absorption spectra of *HT*-P(S)MBET in a chloroform / (s)-(-)-2-methyl-1-butanol mixed solution. (cooling scan)

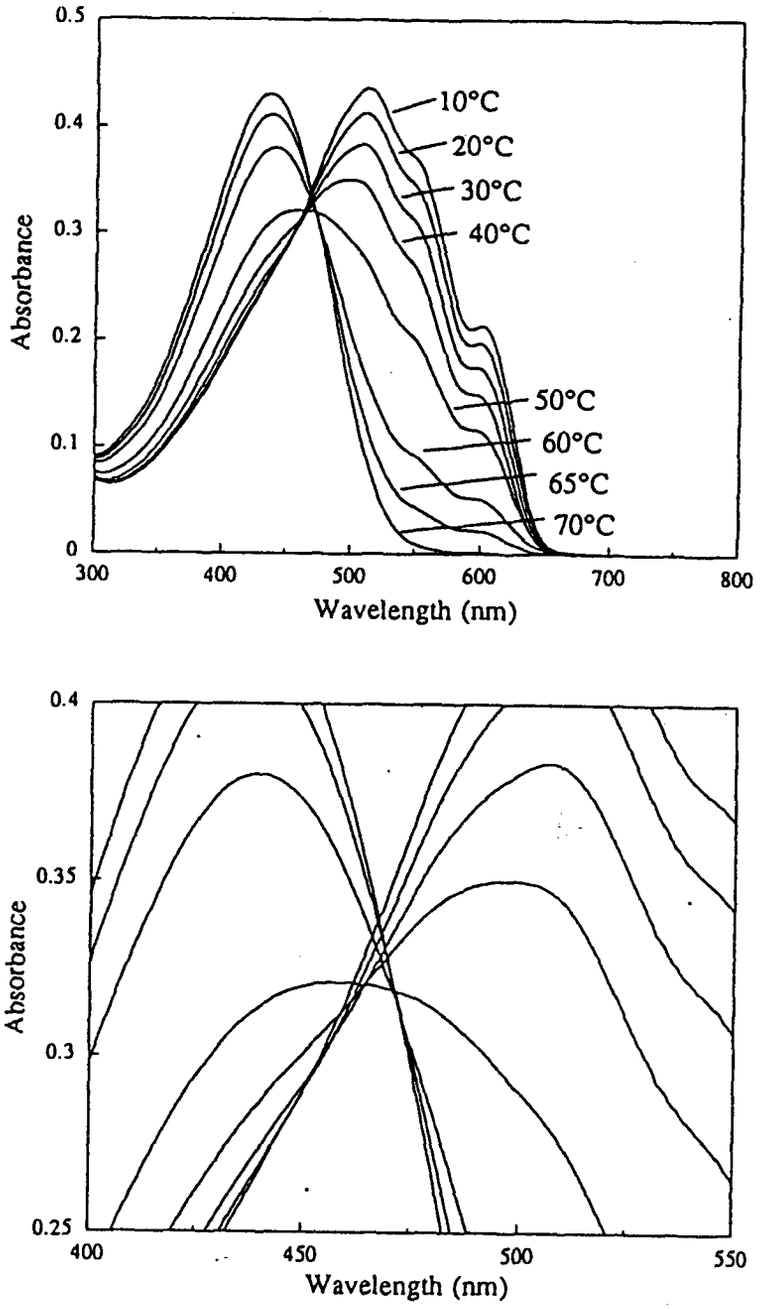

Figure 3.11. Temperature-dependent UV-Vis absorption spectra of *HT*-P(S)MBET in a chloroform / (±)-2-methyl-1-butanol mixed solution. (cooling scan)

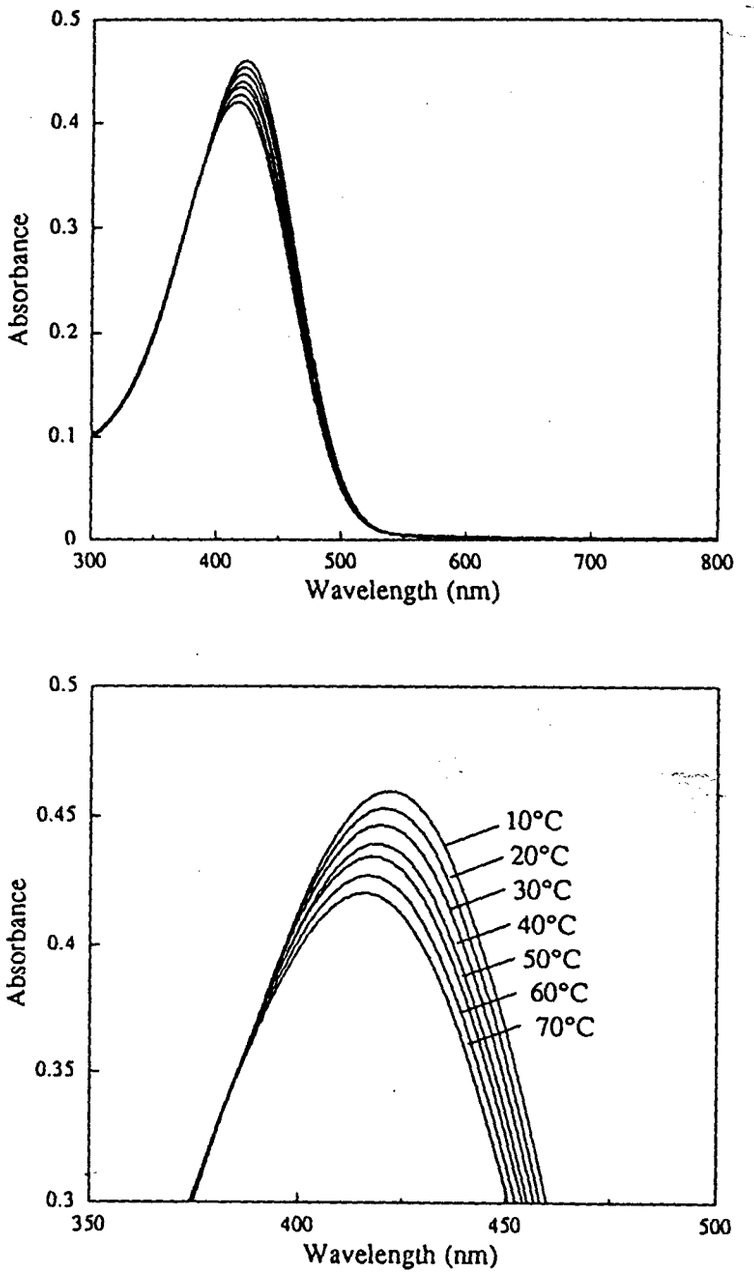

Figure 3.12. Temperature-dependent UV-Vis absorption spectra of *R*-P(S)MBET in a chloroform / (s)-(-)-2-methyl-1-butanol mixed solution. (cooling scan)

References

[1] R.D.McCullough, R.D.Lowe, M.Jayaraman and D.L.Anderson, *J. Org. Chem.*, **58**(1993)904.

[2] R.D.McCullough and R.D.Lowe, *J. Chem. Soc., Chem. Commun.*, (1992)70.

[3] T.-A.Chen and R.D.Rieke, *Synth. Met.*, **60**(1993)175.

[4] T.-A.Chen, X.Wu and R.D. Rieke, *J. Am. Chem. Soc.*, **117**(1995) 233.

[5] P.Buvat and P.Hourqueble, *Macromolecules*, **30**(1997)2685.

[6] A.Iraqi and G.W.Barker, *J.Mater.Chem.*,**8**(1998)25.

[7] W.Luzny, M.Trznadel and A.Pron, *Synthetic Metals.*, **81**(1996)71.

[8] M.Rikukawa, M.Nakagawa, Y.Tabuchi, K.Sanui and N.Ogata, *Synth. Met.*, **84**(1997)233.

[9] M.Rikukawa, M.Nakagawa, H.Abe, K.Sanui and N.Ogata, *Thin Solid Films*, **284-285**(1996)636.

[10] M.Rikukawa, M.Nakagawa, H.Abe, K.Ishida, K.Sanui and N.Ogata, *Thin Solid Films*, **273**(1996)240.

[11] X.Wu, T.-A.Chen and R.D.Rieke, *Macromolecules*, **29**(1996) 7671.

[12] G.Bidan, S.Guillerez and V.Sorokin, *Adv.Mater.*, **8**(2),(1996)157.

[13] R.D.McCullough and S.P.Williams, *J. Am. Chem. Soc.*, **115**(1993) 11608.

[14] R.D.McCullough, S.Tristram-Nagle, S.P.Williams, R.D.Lowe and M.Jayaraman, *J. Am. Chem. Soc.*, **115**(1993)4910.

[15] R.D.McCullough, P.C.Ewbank and R.S.Loewe, *J. Am. Chem. Soc.*, **119**(1997)633.

[16] R.D.McCullough, *Adv.Mater.*, **10**(2)(1998)93.

[17] M.M.Boumann, E.E.Havinga, R.A.J.Janssen and E.W.Meijer, *Mol. Cryst. Liq. Cryst.*, **256**(1994)439.

[18] M.M.Boumann and E.W.Meijer, *Adv.Mater.*, **7**(4)(1995)385.

[19] Y.Tabuchi, master course graduation thesis 1998, Sophia University, Tokyo, Japan.

[20] Alois Fürstner, "Active Metals", VCH Publishers, chapter 4 (1995).

[21] E.Negishi, *Acc. Chem. Res*, **15**(1982)340.

[22] R.Sugimoto, S.Takeda, H.B.Gu and K.Yoshino, *Chem. Express* , **1**(1986)635.

[23] K.Yoshino, S.Hayashi, and R.Sugimoto, *Jpn. J. Appl. Phys.*, **23** (1984)L889.

[24] O.R.Gautun, P.H.J.Carlsen, E.J.Samuelsen and J.Mårdalen, *Synth. Met.*, **58**(1993)115.

[25] P.C.Bizzarri, F.Andreani, C.D.Casa, M.Lanzi and E.Salatelli, *Synth. Met.*, **75**(1995)141.

[26] M.R.Anderson, D.Selese, M.Berggren, H.Järvinen, T.Hjertberg, O.Inganäs, O.Wennerström and J.-E.Österholm, *Macromolecules* , **27**(1994)6503.

[27] M.Sato and H.Morii, *Macromolecules*, **24**(1991)1196.

[28] S.D.D.V.Rughooputh, S.Hotta, A.J.Heeger and F.Wudl, *J.Polum.Sci., Part B: Polym. Phys.*, **25**(1987)1071.

[29] K.Faid, M.Frechette, M.Ranger, L.Mazerolle, I.Levesque, M.Leclerc, T.-A.Chen and R.D.Rieke, *Chem. Mater.*, **7**(1995)1390.

Electrical and Optical Properties of Ultrathin Films

Background

Recently, conducting polymer films with extended π-conjugated electron system have attracted considerable attention because of their important electrical and optical properties. To prepare well-defined ultrathin films, the LB technique is the best method. Conducting polymer LB films are attractive candidates for many applications such as biosensors, ion-sensors, and optoelectronic devices. Therefore, there has been an increased interest shown in the preparation of conducting polymer LB films.

As described in chapter 4, the mixed monolayers of *HT*- P(S)MBET and stearic acid (SA) with different molar ratios could be transferred onto solid substrates as Y-type multilayer films. From the polarized UV-Vis spectra and X-ray diffraction measurements, it was found that the *HT*-P(S)MBET in the LB film has a self-assembling tendency to form a layered structure in which the main chains are oriented parallel to the plane of the substrate and exhibit a tendency to orient along the dipping direction in the LB films.

In reseach reported in this chapter, the electrical conductivities and nonlinear optical (NLO) properties of these LB films were investigated. These LB films are expected to exhibit unique properties which are related to their anisotropic molecular structures. Moreover, investigation of conducting polymer structures, when doped or undoped, is an important goal to a deeper understanding of the structure-property relationships. The influence of doping on the molecular structure has been studied by the use of X-ray diffraction measurements.

The conductivity was measured in order to examine the electrical properties of *HT*-P(S)MBET/SA mixed LB films before and after doping. In-plane conductivity measurements were performed by the four prove method proposed by L. J. Van der Pauw.[1] Contact geometry used thin film conductivity measurements are shown in **Figure 5.1.** Four electrical contacts were made to the outer edges of the film using silver paste. While an electrical current was passed between two leads, the concomitant voltage drop was recorded over the remaining two connections to yield a resistance value (R_1) for that particular geometry. After the first measurement was completed, the leads were changed such that one lead from each of the original parts were switched with the other. In other words, one lead from the voltage-measuring pair was exchanged with one from the current-carrying pair, and the measurement was performed again to give R_2. The following equation was used to determine the resistivity (ρ) of the sample, where t is the sample thickness and f is a constant defined by the second equation.

$$\rho = (\pi\ t / \ln 2)\ [(R_1 + R_2) / 2] \times f\ (R_1 + R_2) \qquad (5.1)$$

$$R_1 / R_2 = (f / \ln 2) \times \text{arccosh}\ \{[\exp(\ln 2 / f)] / 2\} \qquad (5.2)$$

$$\sigma = 1 / \rho \qquad (5.3)$$

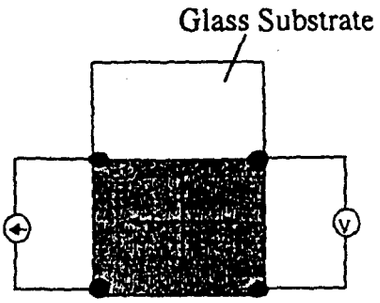

In-plane

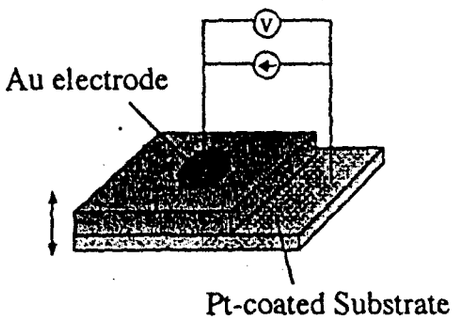

Transverse

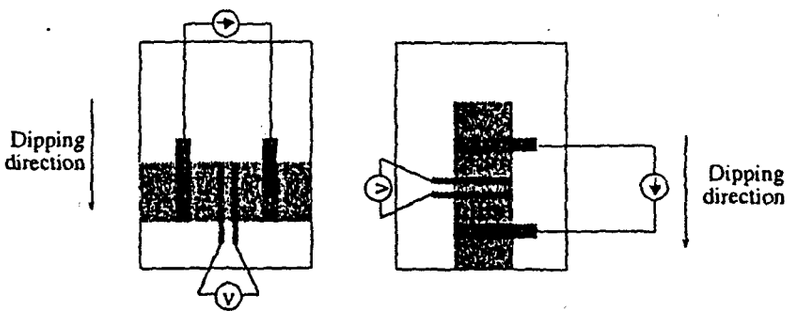

In-plane Anisotropy

Figure 5.1. Schematic view of conductivity measurements by Van der Pauw and ordinary four probe method.

In-plane conductivities of neutral (undoped) films were measured by the Van der Pauw method. The results were presented in **Table 5.1**. In-plane conductivities for the undoped *HT*-P(S)MBET/SA (2/1) LB films were around 10^{-4} S cm^{-1}, which is 2 orders of magnitude higher than that reported for undoped *HT*-PHT/SA (2/1) LB film. Similar result was obtained for ravemic *HT*-P(±)MBET/SA LB films. The reason of this higher conductivity is not clear. It is thought that higher crystallinity of *HT*-P(S)MBET can be attributed to the facilitation of charge transfer. Similar effects were reported by other investigators.[2] In addition, there is another possibility of oxygen doping. The influence of oxygen doping by oxygen [3], moisture [4] or air [5] leads to an increase of the conductivity. It is necessary to measure their conductivities in vacuum.

In the case of the undoped *HT*-P(S)MBET spin-coated films, the conductivities were around 10^{-5} S cm^{-1}. It was found that *HT*-P(S)MBET / SA LB film has higher conductivity than *HT*-P(S)MBET spin-coated film despite the fact that LB films contained non-conducting material, SA. As mentioned in chapter 4, this result is compatible with the observed result that the mixed LB film has lower energy (shorter λ_{max}) than that of the spin-coated film in UV-Vis absorption spectra. It is suggested that the LB manipulation induced the self-organization properties of *HT*-P(S)MBET molecules and extended the conjugation length.

As shown in **Table 5.1**, *HT*-P(S)MBET ultrathin films exhibit enhanced conductivity when compared with the regiorandom *R*-P(S)MBET. In regioregular *HT*-P(S)MBET, steric repulsions between the side chains on the thiophene ring will be decreased, thereby increasing the effective conjugation length between thiophene rings. The conductivity of an *R*-P(S)MBET/SA (2/1) LB film could not be measured.

Before doping

Table 5.1. In-plane conductivity of ultrathin films before doping.

Ultrathin film	Conductivity (S / cm)
HT-P(S)MBET / SA (2 / 1) LB film	5.5×10^{-4}
HT-P(±)MBET / SA (2 / 1) LB film	5.0×10^{-4}
HT-P(S)MBET spin-coated film	3.0×10^{-5}
R-P(S)MBET / SA (2 / 1) LB film	——
R-P(S)MBET spin-coated film	$\sim 10^{-10}$

5-3. Anisotropy of Electrical Conductivity

Optical and electrical anisotropies are among most important properties for various applications of conducting polymers.[6-7] Due to anisotropic molecular structures in the ultrathin films, electrons or holes on the polymer can move only in one direction.

Since the LB technique is based on the anisotropic absorption of amphiphilic molecules onto the air-water interface, it provides a highly ordered structure along the normal axis of the substrate plane. Therefore, the molecules in the LB films are commonly oriented parallel to the plane of the substrate, resulting in the anisotropy between in-plane and transverse properties. Here, I measured the transverse conductivities of undoped (neutral) LB films to compare them with in-plane conductivities.

Transverse conductivity measurements of the LB films were performed by sandwiching the multilayer between two electrodes as shown in **Figure 5.1**. The sandwich structure was attained by depositing the multilayer onto a conductive substrate, a platinum-coated glass slide. The top electrodes were made by vacuum evaporating gold onto the surface of the film. This method not only insured good electrical contact but also provided excellent control of the contact area. However, this process had to be carried out slowly and carefully to avoid damaging the films. The samples were covered by a small mask during the vacuum evaporation process so that the gold deposition produced circular electrodes with areas of 0.071 cm^2. Contact was made to the top electrode by gently lowering a fine gold wire, bent in the shape of a hook, onto the metallic surface. The transverse conductivity was calculated from the values of the applied voltage V and current I using

$$\sigma = It / VA = t / AR \qquad (5.4)$$

where t is film thickness, A is the area of electrode overlap and R is the resistance.

The results are shown in **Table 5.2**. A transverse conductivity of not to more than 10^{-10} S cm^{-1} was observed for 100 layer-thick *HT*-P(S)MBET/SA (2/1) LB film. The conductivity perpendicular to the substrates plane (10^{-10} S cm^{-1}) is six orders of magnitude lower than that parallel to the substrates plane (10^{-4} S cm^{-1}). It is found that there is large electrical anisotropy ($>10^{-6}$) in the mixed LB films.

On the other hand, the anisotropy of in-plane conductivity is also substantial properties of the well-organized films. The anisotropies of in-plane conductivity of LB films is estimated from the ratio of $\sigma_{\parallel}$ (parallel to the dipping direction) to $\sigma_{\perp}$(perpendicular to the dipping direction). Recently, several researchers have reported the in-plane anisotropy in polymer LB films. In most cases, the molecules are preferentially oriented parallel or perpendicular to the dipping direction of the substrate.

In this study, the anisotropy of in-plane conductivity was measured by the four probe in-line technique. Electrodes were made by vacuum evaporating a gold onto the surface of the film. Four electrical contacts were made to the outer edges of the electrode using silver paste. Each conductivity was calculated from the following equation, where d is the distance between voltage terminals and A is the cross section area of the film.

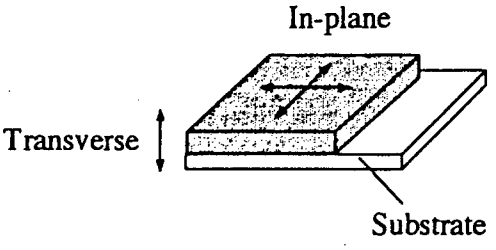

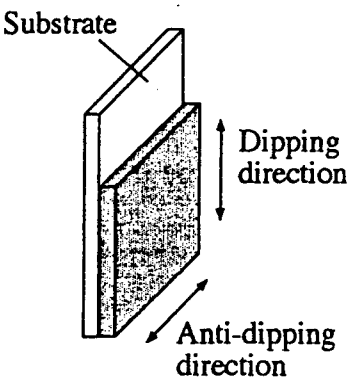

Before doping

Table 5.2. Anisotropies of conductivity of *HT*-P(S)MBET/SA (2/1) LB films measured by four probe method.

Conductivity (S / cm)		Anisotropy
Dipping direction	Anti-dipping direction	Dipping / Anti-dipping
2.4×10^{-4}	1.5×10^{-4}	1.6
In-plane	Transverse	In-plane / Transverse
5.5×10^{-4}	$< 10^{-10}$	$> 10^{6}$

$$\sigma = Id / VA = d / AR \qquad (5.5)$$

As shown in **Table 5.2**, the in-plane conductivity perpendicular to the dipping direction was 2.4×10^{-4} S cm^{-1}, whereas the in-plane conductivity perpendicular to the dipping direction was 1.5×10^{-4} S cm^{-1}. The ratio ($\sigma_{\parallel} / \sigma_{\perp}$) of 1.6 was obtained for the LB films (20 layers) and this value was reproducible. This result proves the preferential alignment of the polymer chains and indicates that the main chains exhibit a tendency to orient along the dipping direction in the LB films. The ratio will become larger as the content of polymer in the film increases. In addition, Chen et al. observed the anisotropy ratio to depend on level of doping.[8] In the doped state, the ratio ($\sigma_{\parallel} / \sigma_{\perp}$) may differ from that of undoped state.

From these results, I conclude that neutral *HT*-P(S)MBET/SA LB films show electrical anisotropies in both transverse and dipping directions. This result is consistent with the structural analysis of the mixed LB films. (see chapter 4) In other words, electrical anisotropies observed in the conductivity measurement clearly bear out the fact that the main chains are oriented parallel to the plane of the substrate and exhibit a tendency to orient along the dipping direction in the LB films.

5-3 Electrical Conductivities of Regioregular Poly(thiophene)s

The in-plane conductivities of doped *HT*-P(S)MBET/SA LB films were also measured by the Van der Pauw method.

HT-P(S)MBET/SA LB films could be rendered electrically conductive by doping with strong acids such as $SbCl_5$, $NOPF_6$ and $FeCl_3$. In this case, doping implies removal of electrons from the polymer chains. Doping was performed by dipping films in a dopant solution. This solution must be a poor solvent (e.g. acetonitrile) for polymers. Doping was accompanied by a drastic color change to a black together with a dramatic increase in the conductivity. (**Figure 5.2**)

Electrical conductivities of these doped films are listed in **Table 5.3**. In spite of dramatic color change from yellow to black, the conductivity of *R*-P(S)MBET ultrathin films could not be measured. The in-plane conductivities of the neutral *HT*-P(S)MBET/SA LB films were in the range of 10^{-4}-10^{-5} S cm^{-1}, whereas the conductivities of doped LB films were in the range of 1-10^{-2} S cm^{-1}. As expected, the conductivity increased as the amount of *HT*-P(S)MBET in the film increases. The highest conductivities are observed when the LB films were doped with $SbCl_5$ from acetonitrile solutions. The conductivity of 1.2 S cm^{-1} was achieved for an *HT*-P(S)MBET/SA (5/1) LB film doped with $SbCl_5$. Solution phase doping with the weak oxidizing agent I_2, on the other hand, results in films with conductivities that are considerably lower. The iodine doped films were rapidly dedoped in air. It suggest that poly(thiophene) has large ionization potential and that the dopant has not fully penetrated the multilayer structure or that iodine only forms a weak charge transfer complex with the polymer backbone. Polymers doped with $FeCl_3$ were relatively more stable than those doped with $NOPF_6$, $SbCl_5$, or I_2, perhaps because of the

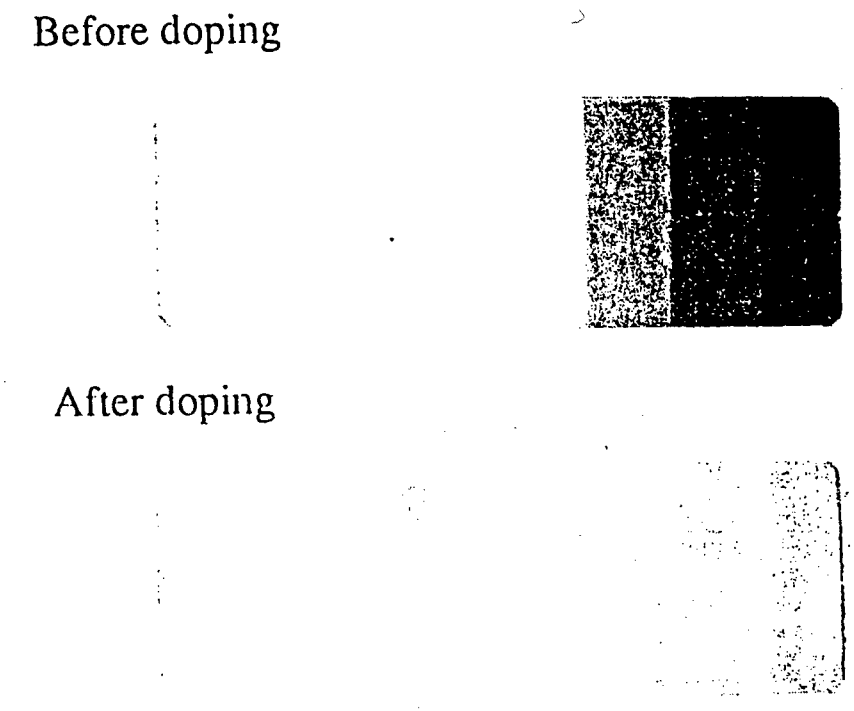

Figure 5.2. Photograph of *HT*-P(S)MBET/SA LB films before and after doping.

After doping

Table 5.3. In-plane conductivity of an *HT*-P(S)MBET/SA (2/1) LB film and an *HT*-P(S)MBET spin-coated film after doping.

Ultrathin film	Dopant [1]	Conductivity (S / cm)
HT-P(S)MBET / SA (2 / 1) LB film [2]	$FeCl_3$	5.8×10^{-2}
2 / 1	$NOPF_6$	7.3×10^{-2}
2 / 1	I_2	3.1×10^{-4}
2 / 1	$SbCl_5$	3.7×10^{-1}
5 / 1	$SbCl_5$	1.2
HT-P(S)MBET spin-coated film [3]	$FeCl_3$	4.3×10^{-3}
	$SbCl_5$	8.9×10^{-3}

1) Solution phase doping with acetonitrile, dopant concentration : 2-3 mg / ml time : 10-12 min.
2) Film thickness : 380 Å (20 layers).
3) Film thickness : 100 Å.

lower flexibility of the $FeCl_4$-doped polymer chains.

In the case of the doped *HT*-P(S)MBET spin-coated films, the conductivities were around 10^{-3} S cm^{-1}. It was found that *HT*-P(S)MBET / SA LB film has higher conductivity than *HT*-P(S)MBET spin-coated film. This result is compatible with the observed result that the mixed LB film has lower transition energy than that of the spin-coated film in UV-Vis spectra. (see chapter 4) It is suggested that the LB manipulation induced the self-organization properties of *HT*-P(S)MBET molecules and extended the conjugation length.

The UV-Vis spectra provide valuable information about the level of oxidation achieved by the various doping processess. **Figure 5.3** shows the UV-Vis spectra of an *HT*-P(S)MBET/SA LB film before and after doping with $SbCl_5$. After doping, the absorption bands (exciton band) for the poly(thiophene) conjugated backbone at 566 and 610 nm are eliminated and new lower energy bands centered at about 820 and 2500 nm appear. These bands are characteristic of a highly oxidized conjugated backbone that is supporting localized defect states in the form of bipolarons.
Significant reductions in the intensity of the interband transition are also observed when the LB films are doped with $NOPF_6$, again suggesting that a high level of oxidation has occurred. Thus, $NOPF_6$ and $SbCl_5$ doped films both contain highly oxidized poly(thiophene) chains. In the case of the doped *HT*-P(S)MBET spin-coated films, bipolarons were similarly induced by dopants.(**Figure 5.4**) Two new bands resulting from transitions of electrons from the valence band to the two newly created bipolaron states are clearly observed.

The influence of doping on the molecular structure has been studied by the use of X-ray diffraction. Comparison of diffraction spectra before and after doping gives information about doping-induced structural changes

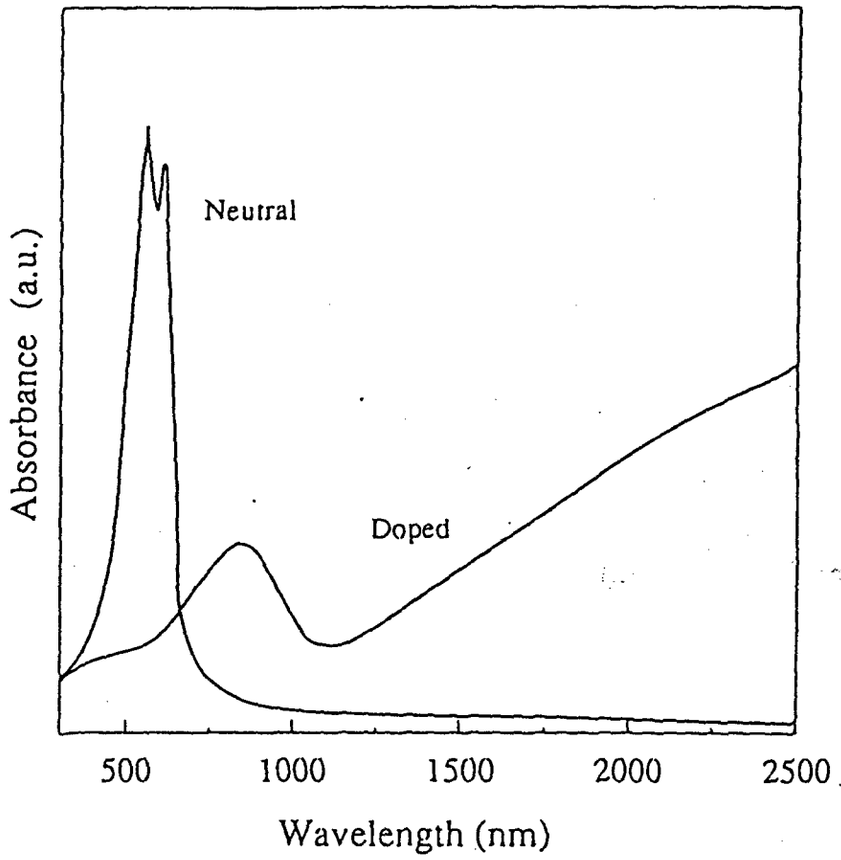

Figure 5.3. UV-Vis spectra of *HT*-P(S)MBET/SA LB films before and after doping with $SbCl_5$.

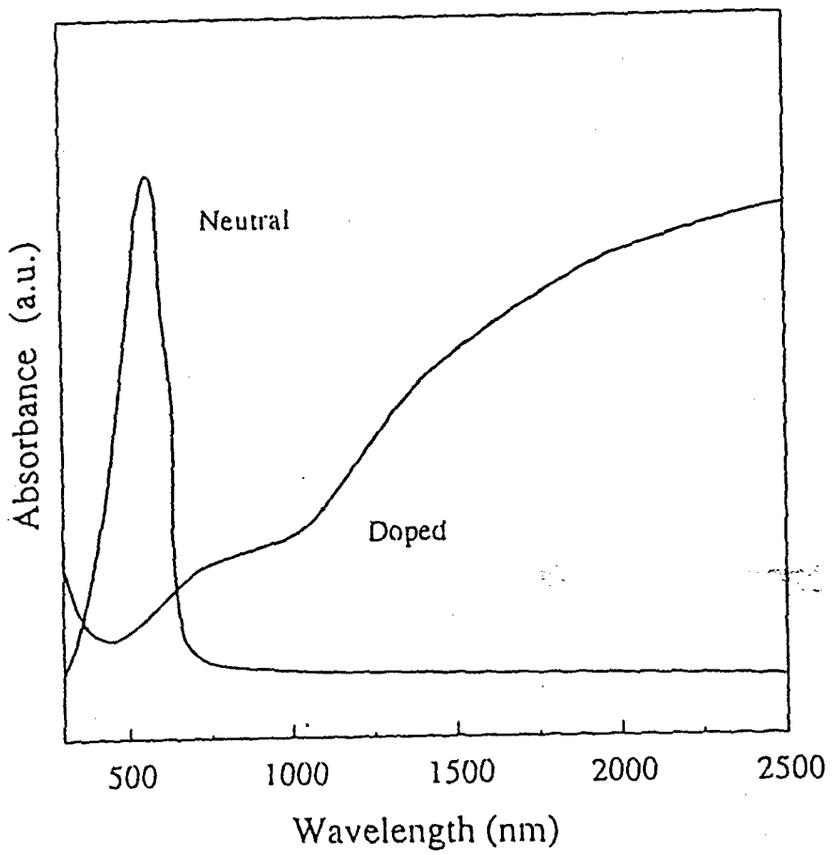

Figure 5.4. UV-Vis spectra of an *HT*-P(S)MBET/SA (2/1) spin-coated films before and after doping with $SbCl_5$.

of the polymer system. [9-15]

The X-ray diffraction patterns of the doped LB films of *HT*-P(S)MBET/SA (2/1) are given in **Figure 5.5**, together with its neutral (undoped) analogue. Before doping, the mixed LB films exhibit a interlayer d-spacing 18 Å (see chapter 4). Doping with $SbCl_5$ almost completely eliminates diffraction peaks and produces a pattern which is devoid of any observable reflection. The strong oxidizing agent $SbCl_5$ may disrupt the molecular organization. In contrast, doping with either $NOPF_6$ and $FeCl_3$ shows a relatively lower intensity of crystalline peaks. Thus the crystallinity of the polymer has significantly decreased upon doping and a new molecular structure has been formed. The position of the first maximum has slightly changed after doping, being shifted to a position indicating higher interplanar distances. In the case of the films doped with $FeCl_3$, we can observe a new reflection at a 2θ angle of 7.9°. This diffraction peak does not appear in pristine films, but it can be seen for all samples doped with $FeCl_3$ even if in spin-coated films. (**Figure 5.6**) Its intensity is proportional to the dopant concentration. One can attribute that the appearance of this peak to the repetition distance associated with the ordering of the dopant anions.[4] Similar changes are also observed when the LB films containing only SA molecules are exposed to $FeCl_3$.

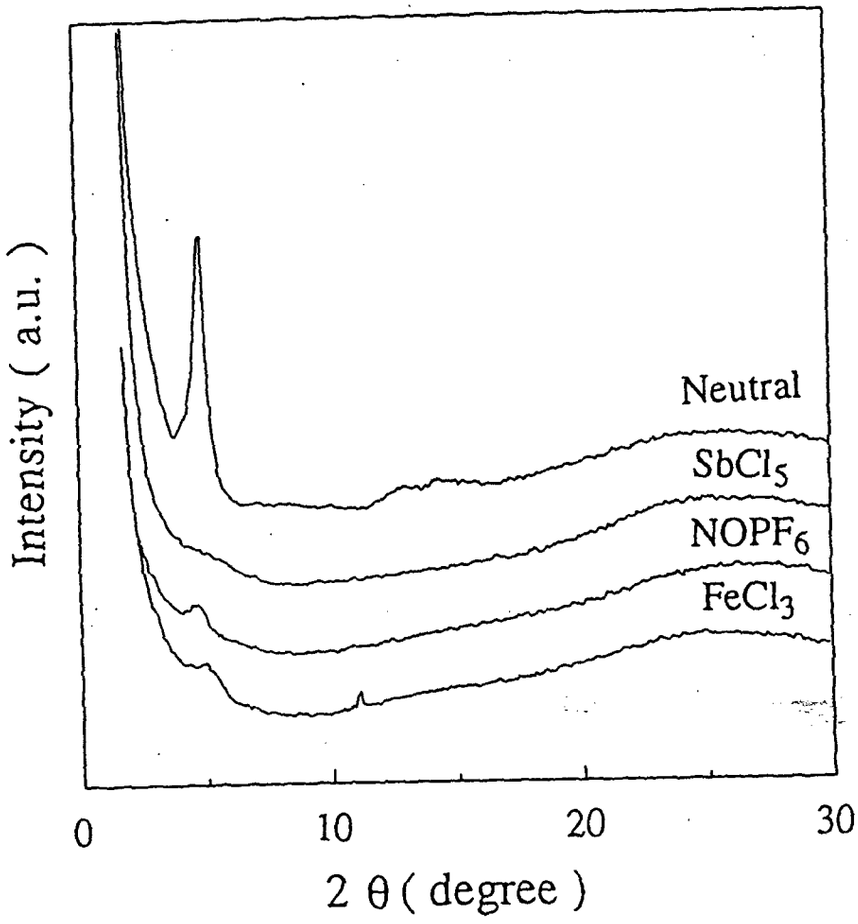

Figure 5.5. X-ray diffraction patterns of *HT*-P(S)MBET/SA (2/1) LB films before and after doping.

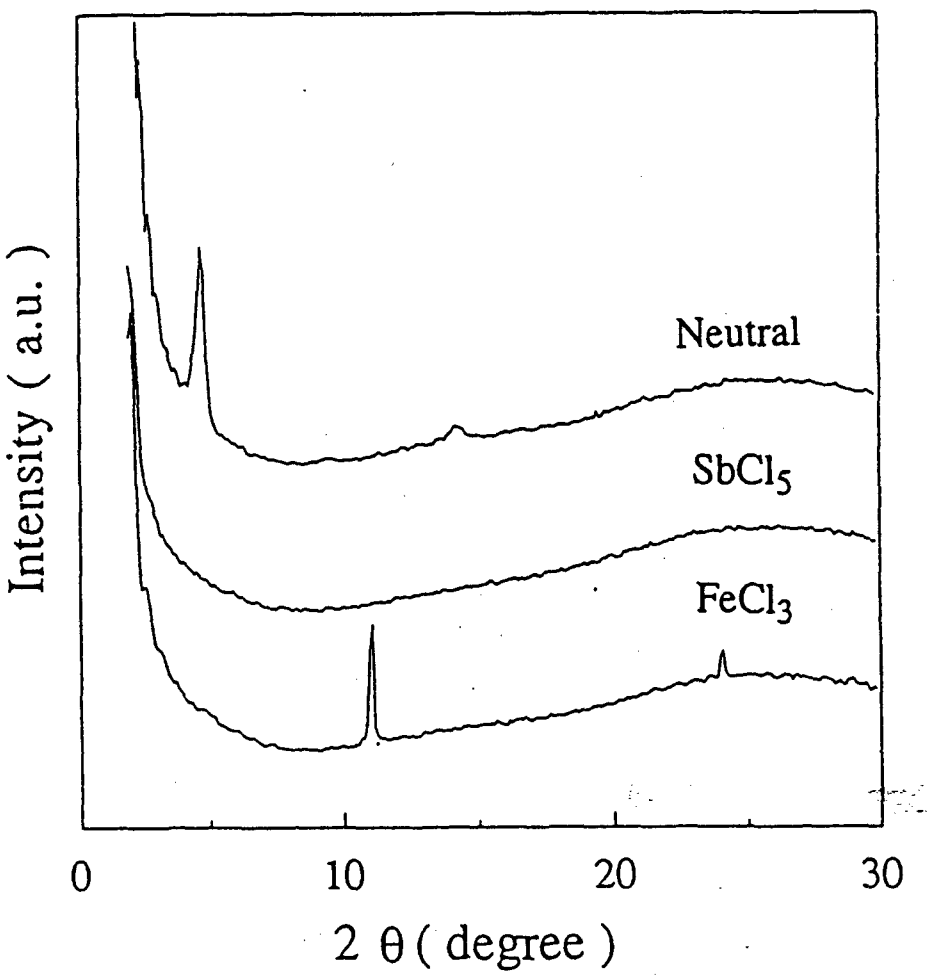

Figure 5.6. X-ray diffraction patterns of *HT*-P(S)MBET/SA (2/1) spin-coated films before and after doping.

5-5. Nonlinear Optical Properties

Thin film fabrication of nonlinear optical (NLO) materials is very important for potential applications as switches and other NLO devices. The electromagnetic field of a laser beam impinging on a material generates an electrical polarization. In the presence of an external electric field **E**, the microscopic polarization **P** induced in an atom or a molecule is given by equation.

$$\mathbf{P} = \chi^{(1)} \cdot \mathbf{E} + \chi^{(2)} \cdot \mathbf{E} \cdot \mathbf{E} + \chi^{(3)} \cdot \mathbf{E} \cdot \mathbf{E} \cdot \mathbf{E} \quad (5.6)$$

Here $\chi^{(1)}$ is the first-order linear optical susceptibility. $\chi^{(2)}$ and $\chi^{(3)}$ are the second-, and the third-order nonlinear optical susceptibilities. The even tensor $\chi^{(2)}$ is zero in centrosymmetric media, whereas the odd tensor $\chi^{(3)}$ does not have any symmetry restrictions. That is to say, symmetry considerations show that the second-order nonlinear optical effects appear only in molecules that lack a center of symmetry, whereas there are no symmetry requirements for third-order nonlinear optical effects. Therefore, a wide variety of materials can be utilized for third-order nonlinear optics.

It is well-known that the π-conjugated polymers have possessed strong third-order NLO effects among many organic materials because of the large π-electron contribution to the electrical susceptibility.[14-15] The NLO properties are characterized through the measurements of the third-order nonlinear susceptibility $\chi^{(3)}$. Polymers with large nonlinear optical susceptibilities are likely to play a major role in the rapidly growing

area of photonics. Magnitudes were typically observed in ... conjugated polymers range from 10^{-12} to 10^{-9} esu. In this study, the third-order nonlinear susceptibility of an *HT*-P(S)MBET/SA LB film and an *HT*-P(S)MBET spin-coated film were measured around exciton resonance using degenerate four wave mixing (DFWM). The schematic view of DFWM measurement is shown in **Figure 5.7**. DFWM is one of the most important technique to provide information on the magnitude and the response of third-order nonlinearity. Many reports on the aspects and analysis of the DFWM technique have been published from the late 1970s. [16-19]

In this study, for the first time the third-order nonlinear susceptibility of the mixed LB films can be obtained by increasing the content of π-conjugated polymers in the LB films.[20] **Figure 5.8** shows the absorption spectrum and the $|\chi^{(3)}|$ spectrum of the neutral *HT*-P(S)MBET/ SA (10/1) LB film (7 layers) at 8K. The LB films exhibit a large absorption in the visible region, which is associated with exciton band and its vibronic sidebands. Each absorption peak at 8K becomes clearer than at room temperature and shifts to the longer wavelength side, because the backbone conformation can be made more regular when the thermal motion of sidechains is suppressed. The $|\chi^{(3)}|$ values of the LB film were greatly enhanced when the harmonic wavelength was in the absorption region. The observed value of $|\chi^{(3)}|$ in the *HT*-P(S)MBET / SA LB film was in the order of 10^{-8} esu. The maximum $|\chi^{(3)}|$ in the *HT*-P(S)MBET/SA LB film was 3.7×10^{-7} esu, which was approximately ten-fold larger than that in an *HT*-P(S)MBET spin-coated film. This is one of the highest values found so far for poly(thiophene) derivatives. Similar result was obtained

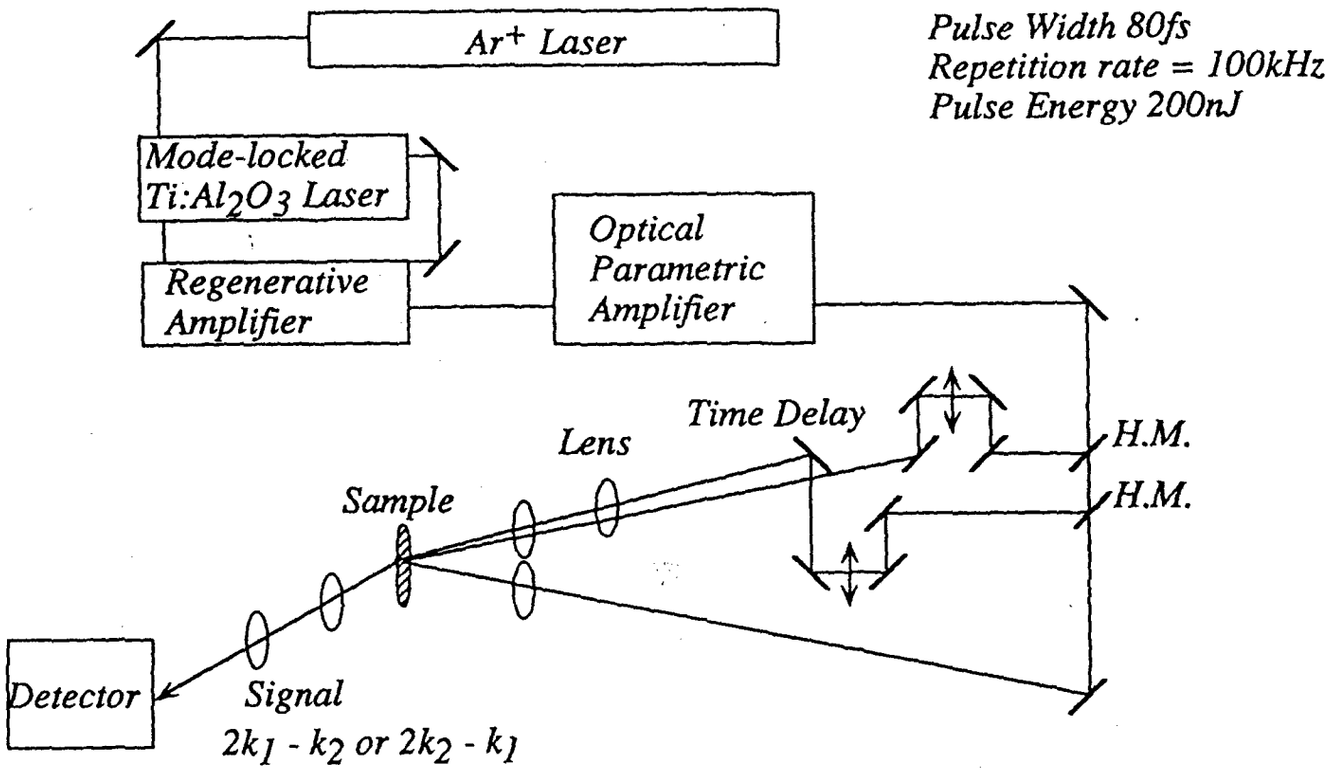

Figure 5.7. Schematic view of degenerate four wave mixing (DFWM).

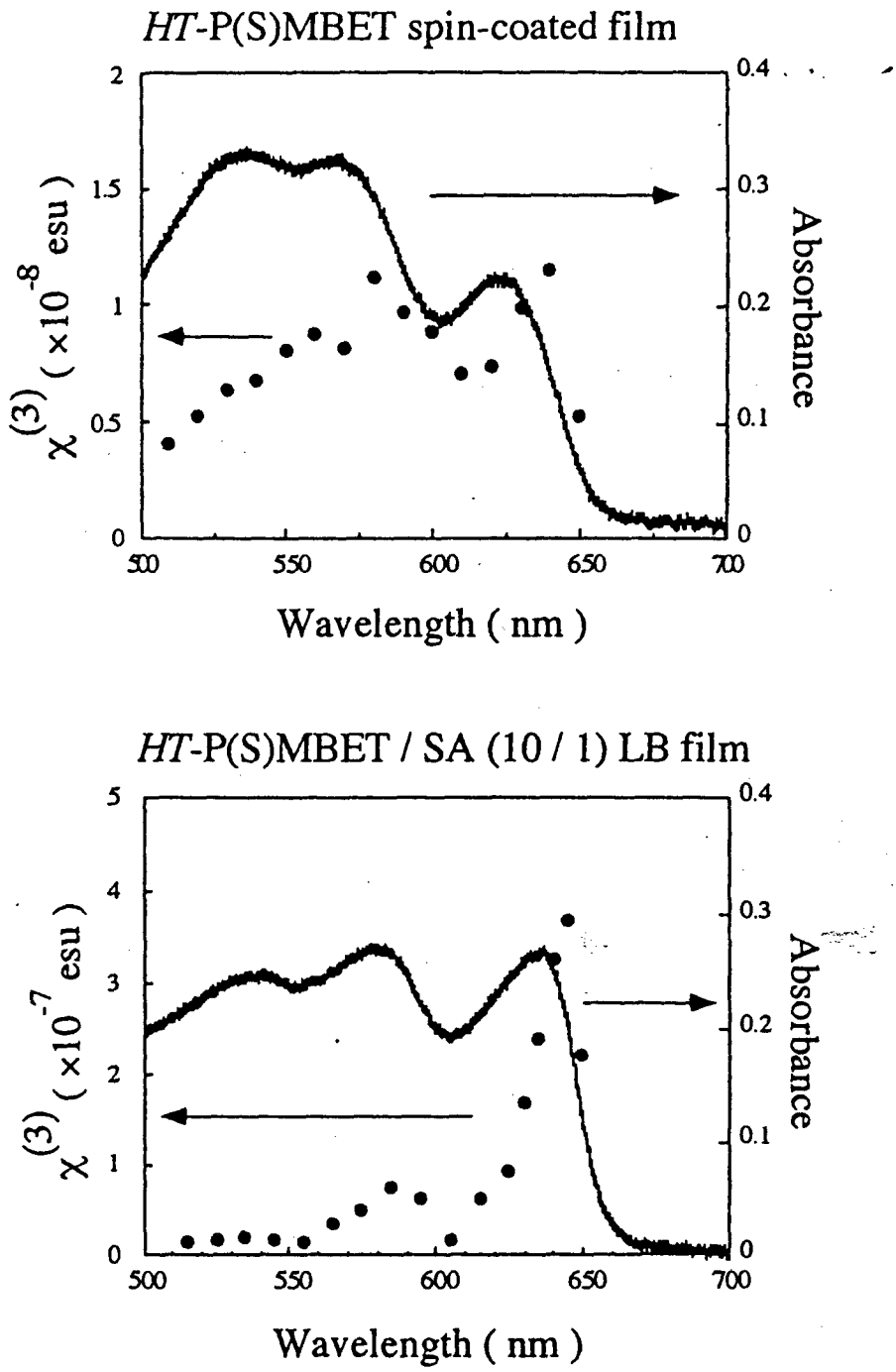

Figure 5.8. $|\chi^{(3)}|$ data of an *HT*-P(S)MBET spin-coated film and an *HT*-P(S)MBET/SA (10/1) LB film measured by degenerate four-wave mixing (DFWM) at 8K.

for the *HT*-P(±)MBET/SA LB film. The maximum $|\chi^{(3)}|$ in the *HT*-P(±)MBET/SA (10/1) LB film was 3.7×10^{-7} esu. It was suggested that NLO property are little affected by chirality of the side chains.

By measuring the UV-Vis spectra and $|\chi^{(3)}|$ spectra, we can calculate the effective conjugation length of the polymer according to other reports.[21-22] As stated before, the effective conjugation length is independent of its molecular weight. The effective conjugation length is the distance that delocalized π-electrons can move. (**Figure 1.4**) The effective conjugation length of the polymer is one of the most important factors that govern the magnitude of the third-order optical nonlinearity. [23-24] In the spin-coated films, the conjugation length was determined to be 20 thiophene rings, while LB films have a conjugation length of 36 thiophene rings (72π-electrons). [20]

From these results above, it is concluded that the LB manipulation induced the self-organization properties of *HT*-P(S)MBET molecules and extend the conjugation lengths.

References

[1] L. J. Van der Pauw, *J. Philips Res. Rep.*,**13**(1958)1.

[2] M.Hatano., *Kogyo Kagaku Zasshi*, **65**(1962)723.

[3] C.Väterlein, B.Ziegler, W.Gebauer, H.Neureuter, M.Stoldt, M.S. Weaver, P.Bäuerle, M.Sokolowski, D.D.C.Bradley and E.Umbach, *Synth.Met.*, in press.

[4] A.Czerwinski, H.Zimmer, A.Amer, S.Van Pham Chiem. Pons and H.B.Mark, *J. Chem. Soc., Chem. Commun.*, (1985)1158.

[5] G.Horowiz, X.Peng, D.Fichhou and F.Garnier, *Appl.Phys.Lett.*, **67**(1990)258.

[6] V.Cimrova, M.Remmers, D.Neher and G.Wegner, *Adv.Mater.*, **8**(2) (1996)146.

[7] A.Bolognesi, G.Bajo, J.Paloheimo, T.Östergård and H.Stubb, *Adv. Mater.*, **9**(2)(1997)121.

[8] Y.-C.Chen, K.Aakagi and H.Shirakawa, *Synthetic Metals.*, **14** (1986)173.

[9] W.Luzny and A.Pron, *Synthetic Metals.*, **69**(1995)337.

[10] W.Luzny, S.Niziol, G.Straczynski and A.Pron, *Synthetic Metals.*, **62** (1994)273.

[11] W.Luzny, M.Trznadel and A.Pron, *Synthetic Metals.*, **81**(1996)71.

[12] K.Tashiro, Y.Minagawa, M.Kobayashi, S.Moriat, T.Kawai and Y.Yoshino, *Jpn.J.Appl.Phys.*, **33**(1994)L1023.

[13] M.J.Winokur, P.Wamsley, J.Moulton, P.Smith and A.J.Heeger, *Macromolecules*, **24**(1991)3812.

[14] T.Sugimoto, T.Wada and H.Sasabe, *Synthetic Metals.*, **28**(1989) C323.

[15] C.L.Callender, L.Robitallie and M.Leclerc. *Opt.Eng.*, **32**(1993)

2246.

[16] S.A.Jenekhe and S.K.Lo. S.R.Fiom, *Appl.Phys.Lett.*, **54**(25)(1989) 2524.

[17] D.N.Rao, J.Swiatkiewicz, P.Chopra, S.K.Ghoshal and P.N.Prasad, *Appl.Phys.Lett.*, **48**(18)(1986)1187.

[18] S.A.Jenekhe, W-C.Chen and S.K.Lo.S.R.Fiom, *Appl.Phys.Lett.*, **57**(2)(1990)126.

[19] W.Schrof, S.Rozouvan, E.V.Keuren, D.Horn, J.Schmitt and G. Decher, *Adv.Mater.*, **3**(4)(1998)338.

[20] S.Kishino, Y.Ueno, K. Ochiai, M. Rikukawa, K. Sanui, T.Kobayashi, H.Kunugita and K.Ema, *Phys. Rev.* B, **58**(20)(1998)13430.

[21] K. Sakurai, *Phys. Rev.* B, **56**(15)(1997)9552.

[22] R.W. Boyd, " Nonlinear Optics ", Academic Press.

[23] T.Bjørnholm, D.R.Greve, T.Geisler, J.C.Peterson, M.Jayaraman and R.D.McCullough, *Adv.Mater.*, **8**(1996)920.

[24] H.Kawahara, Y.Ueno, N.Abe, S.Kishino, K.Ema, M.Rikukawa, Y.Tabuchi and N.Ogata, *Optical Review*, **14**(1997)118.

Conclusion

Regioregular poly(alkylthiophen)s having head-to-tail structures were synthesized from 3-[2-((S)-2-methylbutoxy)ethyl]thiophene according to a modified Rieke method for the first time. Structural analyses of the obtained poly(thiophene)s indicated that the regioregularity strongy affected the conjugated structure of main polymer chains.

Thus, opto-electronic properties of the poly(thiophene)s depended on the regioregularity of the polymers and both electrical conductivity and third order non-liniarity of head-to-tail poly(thiophene)s were enhanced in comparison with regiorandom poly(thiophene)s owing to the increased conjugation lengths.

Acknowledgement

I thank to AFOSR for the support of this research project during three years from 1996 to1999..